Nonisothermal Stirred-Tank Reactor with Irreversible Exothermic Reaction A → B : 2. Nonlinear Phenomena

CHAPTER *in* LECTURE NOTES IN CONTROL AND INFORMATION SCIENCES · OCTOBER 2007

Impact Factor: 0.25 · DOI: 10.1007/978-3-540-73188-7_8

2 AUTHORS:

Manuel Pérez-Polo
University of Alicante
48 PUBLICATIONS **213** CITATIONS
SEE PROFILE

P. Albertos
Universitat Politècnica de València
200 PUBLICATIONS **1,235** CITATIONS
SEE PROFILE

NONISOTHERMAL STIRRED-TANK REACTOR WITH IRREVERSIBLE EXOTHERMIC REACTION A→B
2. NONLINEAR PHENOMENA

Manuel Pérez Polo. Department of Física Ingeniería de Sistemas y Teoría de la Señal. Escuela Politécnica Superior. Alicante University. Campus de San Vicente, Alicante 03071, Spain. Tel: 34-965909673; Fax 34-965909750. E-mail: manolo@disc.ua.es.

Pedro Albertos Pérez. Department of Systems Engineering and Control, E.T.S.I.I. Universidad Politécnica de Valencia Camino de Vera s/n, Valencia Spain. Fax: 34 963879579. E-mial: pedro@aii.upv.es

Abstract

In this chapter, the non-linear dynamics of a nonisothermal CSTR where a simple first order reaction takes place is considered. From the mathematical model of the reactor without any control system, and by using dimensionless variables, it has been corroborated that an external periodic disturbance, both inlet stream temperature and coolant flow rate, can lead to chaotic dynamics. The chaotic behavior is analyzed from the sensitivity to initial conditions, the Lyapunov exponents and the power spectrum of reactant concentration. Another interesting case is the one researched from the self-oscillating regime, showing that a periodic variation of coolant flow rate can also produce chaotic behavior. Finally, steady-state, self-oscillating and chaotic behavior with two PI controllers have been investigated. From different parameters of the PI controllers, it has been verified that a new self-oscillating regime can appear. In this case, the saturation in a control valve gives a Shilnikov type homoclinic orbit, which implies chaotic dynamics. The existence of a new set of strange attractors with PI control has been analyzed from the initial conditions sensitivity. An Appendix to show a computationally simple form to implement the calculation of Lyapunov exponents is also presented.

Keywords: Reactor; Non-linear dynamics; Regular; Self-oscillating; Chaotic; PI control; Homoclinic orbit.

1. Introduction

It is well known that self-oscillation theory concerns the branching of periodic solutions of a system of differential equations at an equilibrium point. From Poincaré, Andronov (Andronov, Vitt and Khaikin, 1966) up to the classical paper by Hopf (Hopf, 1942, Marsden and McCraken, 1976), non-linear oscillators have been considered in many contexts. An example of the classical electrical non-oscillator of van der Pol can be found in the paper of Cartwright (Cartwright, 1945). Poore and later Uppal (Uppal, 1974) were the first researchers who applied the theory of nonlinear oscillators to an irreversible exothermic reaction A → B in a CSTR. Afterwards, several examples of self-oscillation (Andronov-Poincaré-Hopf bifurcation) have been studied in CSTR and tubular reactors. Another example taken from mechanics and electronics

can be found in Guckenheimer and Holmes, 1983; Tomita, 1986; Wiggins, 1988, 1990; Lichtnberg and Lieberman, 1992; Seydel, 1994.

The experiments and the simulation of CSTR models have revealed a complex dynamic behavior that can be predicted by the classical Andronov-Poincaré-Hopf theory, including limit cycles, multiple limit cycles, quasi-periodic oscillations, transitions to chaotic dynamic and chaotic behavior. Examples of self-oscillation for reacting systems can be found in Andronov, Vitt and Khaikin, 1966; Uppal, Ray and Poore, 1974; Marsden and McCraken, 1976; Vaganov, Samoilenko and Abranov, 1978; Zhabotinsky and Rovinskii, 1984; Mankin and Hudson, 1984; Planeaux and Jensen, 1986; Teymour and Ray, 1989; Teymour, 1997, Pérez,Font and Montava, 2002. The paper of Mankin and Hudson in which a CSTR with a simple reaction $A \rightarrow B$ takes place, shows that it is possible to drive the reactor to chaos by perturbing the cooling temperature. In the paper by Pérez, Font and Montava, it has been shown that a CSTR can be driven to chaos by perturbing the coolant flow rate. It has been also deduced, by means of numerical simulation, that periodic, quasi-periodic and chaotic behaviors can appear.

More recently, the problem of self-oscillation and chaotic behavior of a CSTR with a control system has been considered in others papers and books (Kubickova, Kubicek and Marek, 1987; Pellegrini and Biardi, 1990; Dolnik, Banks and Epstein, 1997; Alvarez-Ramirez, Suarez and Femat, 1997; Soroush, 1997; Alvarez-Ramirez,Femat and Gonzalez-Trejo, 1998; Femat, 2000; Kurtz, Yan Zhu and Henson, 2000; Pérez and Albertos, 2004). In the previously cited papers, the control strategy varies from simple PID to robust asymptotic stabilization. In these papers, the transition from self-oscillating to chaotic behavior is investigated, showing that there are different routes to chaos from period doubling to the existence of a Slinikov's homoclinic orbit (Shilnikov, 1965, 2001). It is interesting to remark that in an uncontrolled CSTR with a simple irreversible reaction $A \rightarrow B$ it does not appear any homoclinic orbit with a saddle point. Consequently, Melnikov method cannot be applied to corroborate the existence of chaotic dynamic (Wiggins, 1988).

In the present chapter, steady state, self-oscillating and chaotic behavior of an exothermic CSTR without control and with PI control is considered. The mathematical models have been explained in part one, so it is possible to use a simplified model and a more complex model taking into account the presence of inert. When the reactor works without any control system, and with a simple first order irreversible reaction, it will be shown that there are intervals of the inlet flow temperature and concentration from which a small region or lobe can appears. This lobe is not a basin of attraction or a strange attractor. It represents a zone in the parameters-plane inlet stream flow temperature-concentration where the reactor has self-oscillating behavior, without any periodic external disturbance.

In this situation, a periodic variation of coolant flow rate into the reactor jacket, depending on the values of the amplitude and frequency, can drive to reactor to chaotic dynamics. With PI control, and taking into account that the reaction is carried out without excess of inert (see part 1), it will be shown that it the existence of a homoclinic Shilnikov orbit is possible. This orbit appears as a result of saturation of the control valve, and is responsible for the chaotic dynamics. The chaotic dynamics is investigated by means of the eigenvalues of the

linearized system, bifurcation diagram, divergence of nearby trajectories, Fourier power spectra, and Lyapunov's exponents.

2. CSTR models equations for a simple reaction A → B

Let us assume that an irreversible exothermic reaction A → B is carried out in a CSTR, as shown in Figure 1. The cooling jacket surrounding the reactor removes the reaction heat. Perfectly mixed and negligible heat losses are assumed. The jacket is assumed to be perfectly mixed and the mass of the metal walls is considered negligible.

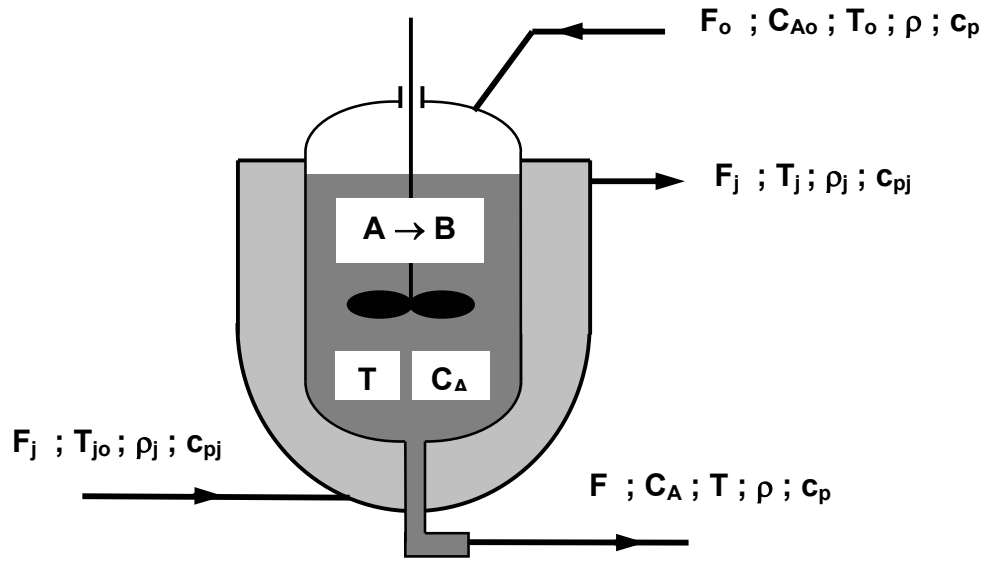

Fig. 1. Perfectly mixed CSTR

The reactor model without control includes the following equations (see part 1):

$$\left.\begin{aligned}
\frac{dC_A}{dt} &= \frac{F_0}{V}(C_{A0}-C_A)-\alpha\cdot C_A\cdot e^{-E/RT}\\
\frac{dT}{dt} &= \frac{F_0}{V}(T_0-T)+\frac{(-\Delta H_R)\alpha}{\rho\cdot c_p}C_A\cdot e^{-E/RT}-\frac{UA}{\rho\cdot c_p V}(T-T_j)\\
\frac{dT_j}{dt} &= \frac{F_j}{V_j}(T_{j0}-T_j)+\frac{UA}{\rho_j\cdot c_{pj}V_j}(T-T_j)
\end{aligned}\right\} \qquad (1)$$

In order to simplify the mathematical model of the reactor, the following dimensionless variables are introduced

$$\tau=\frac{F_0 t}{V}\ ;\ x=\frac{C_A}{C'_{A0}}\ ;\ \mathrm{x}_0=\frac{C_{A0}}{C'_{A0}} \qquad (2)$$

where C'_{A0} is the initial concentration of reactant A in the reactor. The temperatures are transformed to dimensionless variables from the following equations:

$$\frac{1}{y}=\frac{E}{RT}\ ;\ \frac{1}{z}=\frac{E}{RT_j}\ ;\ \frac{1}{y_0}=\frac{E}{RT_0}\ ;\ \frac{1}{y_{j0}}=\frac{E}{RT_{j0}} \tag{3}$$

Substituting the values of $t, C_A, C_{A0}, T, T_j, T_0, T_{j0}$ from Eq (2) and 3 into Eq (1), the mathematical model of the reactor in dimensionless variables can be written as:

$$\left.\begin{aligned}\frac{dx}{d\tau}&=x_0-x-c_0xe^{-1/y}\\ \frac{dy}{d\tau}&=y_0-y+c_1xe^{-1/y}-c_2(y-z)\\ \frac{dz}{d\tau}&=c_3(z_{jo}-z)+c_4(y-z)\end{aligned}\right\} \tag{4}$$

where the parameters c_0, c_1, c_2, c_3, c_4 are defined from the following equations:

$$\begin{gathered}c_0=\frac{V}{F_0}\alpha\ ;\ c_1=\frac{VR(-\Delta H_R)C'_{A0}}{F_0E\rho\cdot c_p}\alpha\ ;\ c_2=\frac{UA}{\rho\cdot c_pF_0}\\ c_3=\frac{VF_j}{V_jF_0}\ ;\ c_4=\frac{\rho\cdot c_pV}{\rho_jc_{pj}V_j}c_2\end{gathered} \tag{5}$$

Typical values of the reactor parameters, to be used in the following discussion, are shown in Table 1. These values are different respect to ones used in chapter 1 because they represent another first order reaction.

TABLE 1
PARAMETER VALUES OF THE REACTOR FOR THE REACTION A → B

Variable	Description	Value
V	Reactor volume (m^3)	1.3592
V_j	Jacket volume (m^3)	0.0849
C_{A0}	Reactant concentration inlet stream (kmol A/m^3)	8
F_0	Volumetric flow rate for the inlet stream (m^3/h)	1.1326
F_j	Volumetric flow rate of cooling water (m^3/h)	1.4130
α	Preexponential factor. Arrhenius law (h^{-1})	7.08×10^{10}
E	Activation energy (kJ/kmol)	69,631
A	Heat transfer area (m^2)	23.255
U	Overall heat transfer in the jacket kJ/(h.m^2.°C)	3068.5
T_0	Inlet stream temperature (K)	294.4
T_{jo}	Inlet stream cooling water temperature (K)	294.4
R	Perfect-gas constant kJ/kmol.K	8.314
$-\Delta H_R$	Enthalpy of reaction (Kj/kmol)	69,828
C_p	Heat capacity inlet and out streams (kJ/kg.K)	3.142
C_{pj}	Heat capacity of cooling water (kJ/kg.K)	4.189
ρ	Density of the inlet and out streams (kg/m^3)	800
ρ_j	Density of cooling water (kg/m^3)	1000

Using these parameters, Eqs (4) can be simplified considering the dimensionless time constant for the reactor τ_y and the dynamics of the jacket τ_z whose values are:

$$\tau_y = \frac{1}{1+c_2} \;;\; \tau_z = \frac{1}{c_3 + c_4} \tag{6}$$

If $\tau_y >> \tau_z$ the jacket's dynamic can be neglected. Therefore, the jacket's temperature is very close to the reactor temperature, and the dimensionless temperature in the jacket z can be removed from equation (4) as follows:

$$z = \frac{c_3 z_{j0} + c_4 y}{c_3 + c_4} \tag{7}$$

Remark 1. The assumption $\tau_y >> \tau_z$ is verified for small reactors. See Figure 7 and Table 2 of part 1.

Substituting Eq (7) into Eq (4) the simplified equations of the reactor are obtained:

$$\left.\begin{aligned} \frac{dx}{d\tau} &= x_0 - x - c_0 x e^{-1/y} \\ \frac{dy}{d\tau} &= y_0 - y + c_1 x e^{-1/y} - c_5 (y - z_{j0}) \end{aligned}\right\} \tag{8}$$

where $c_5 = (c_2 c_3)/(c_3 + c_4)$. Eqs. (8) are used to investigate the existence of self-oscillating and chaotic behavior.

3. Self-oscillation and chaotic behavior of a CSTR without feedback control

Equations (4) and (8) can be used to simulate the reactor at point P_3 of Figure 5 in part 1. Remember that point P_2 is unstable, so if the initial conditions are those corresponding at this point, it is easy to show (Luyben, 1990, Stephanopoulos, 1992), the reactor evolves to points P_1 or P_3. Then, two forcing actions on the reactor are considered: 1) when the coolant flow rate and the inlet stream temperature are varied as sine waves, and 2) reactor being in self-oscillating mode, an external disturbance in the coolant flow rate can drive it to chaotic behavior.

3.1 Chaotic behavior with double external periodic disturbance

It is well known that a nonlinear system with an external periodic disturbance can reach chaotic dynamics. In a CSTR, (Mankin and Hudson (1984)) it has been shown that the variation of the coolant temperature, from a basic self-oscillation state makes the reactor to change from periodic behavior to chaotic one. On the other hand, in the paper by Pérez, Font and Montava (2002), it has been shown that it is possible to reach chaotic behavior from an external sine wave disturbance of the

coolant flow rate. Note that a periodic disturbance can appear, for instance, when the parameters of the PID controller which manipulates the coolant flow rate are being tuned by using the Ziegler-Nichols rules. The chaotic behavior is difficult to obtain from normal operating conditions, but it is possible to obtain at the start and shutdown operations.

In order to investigate this behavior, we consider the mathematical model of the reactor given by Eqs (1) or (4), and it is assumed that the reactor is at the steady state corresponding at point P_3 of Figure 2 in part 1. The disturbances of the dimensionless inlet stream temperature and the coolant flow rate are the following:

$$y_0 \rightarrow y_0 + \frac{RA_t}{E} sin(\omega \cdot \tau)$$
$$F_j \rightarrow F_j + A_f sin(\omega \cdot \tau) \qquad (9)$$

where A_t and A_f are the amplitudes of the inlet stream temperature and coolant flow rate external disturbances respectively, and ω the dimensionless frequency. Figure 2 shows chaotic oscillations of concentration and reactor temperature, and Figure 3 shows the strange attractor in the C_A-T plane.

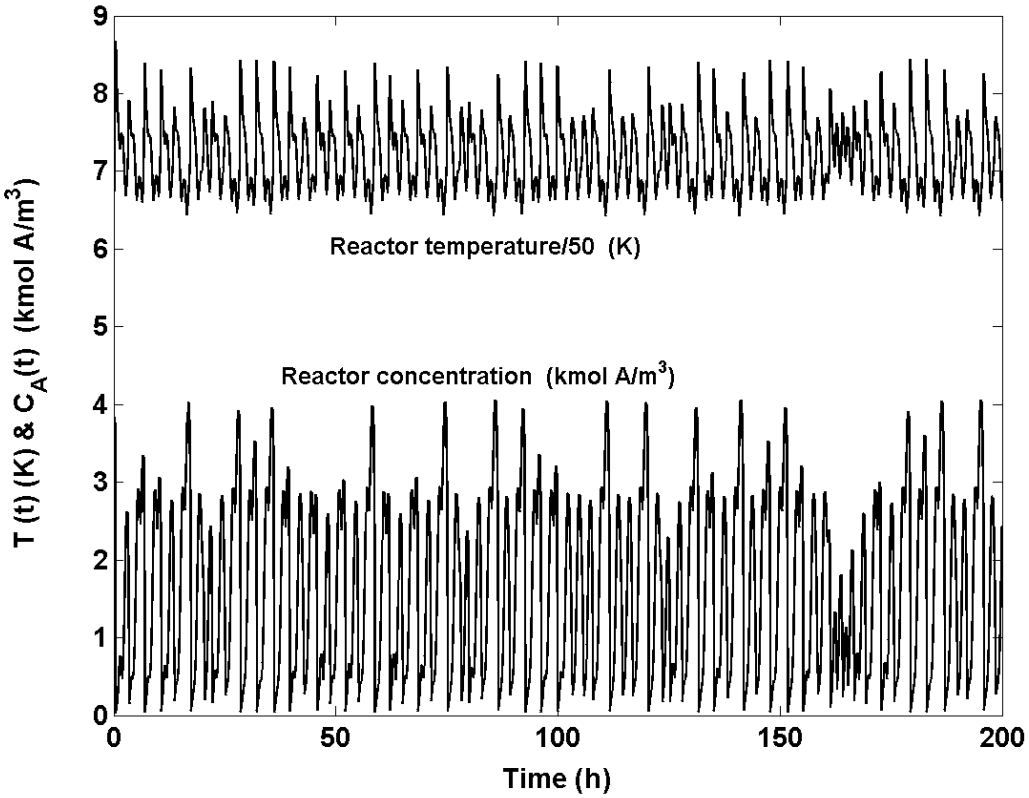

Fig. 2. Chaotic oscillations for three-dimensional model Eq. (1)-(4). C'_{Ao} = 8 kmol/m^3. A_t = 111.1 K; A_f = 0.849 m^3 /h; ω = 5 rad/h

Figure 4 shows a pattern of the concentration when the chaotic motion is established as well as the evolution of the deviation from two very close initial conditions. Note that nowadays it is very difficult to

prove rigorously that a strange attractor is chaotic. In accordance with Wiggins, 1990, a nonlinear system has chaotic dynamics if:

1. It has sensitive dependence on initial conditions, i.e. two very close initial conditions diverge with time.
2. The orbits are dense in a state space region i.e. the orbits fills the phase space zone of the strange attractor Ω
3. The orbits are topologically transitive in Ω i.e. for any two open sets Ω_1 , $\Omega_2 \subset \Omega$ there is a time from which any orbit starting at Ω_1 ends at Ω_2.

While the conditions 1,2 can be verified approximately by simulation, proving the condition 3 is very difficult. Note that in many studies of chaotic behavior of a CSTR, only the conditions 1,2 are verified, which does not imply chaotic dynamics, from a rigorous point of view. Nevertheless, the fulfillment of conditions 1,2, can be enough to assure the long time chaotic behavior i.e. that the chaotic motion is not transitory. From the global bifurcations and catastrophe theory other chaotic behavior can be considered throughout the disappearance of a saddle-node fixed point (Glendinning, 1994; Shilnikov et al. 2001; Ott, 2002).

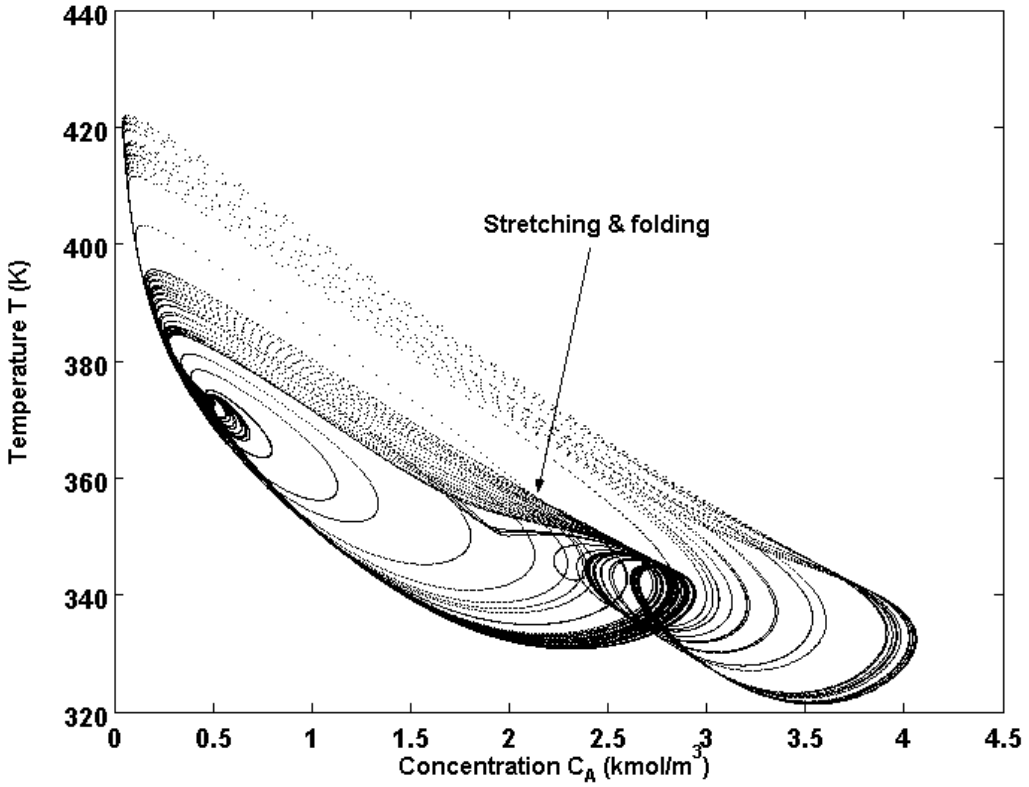

Fig. 3. Strange attractor for model (1)-(4) driven by equation (9).

Remark 2. Note that Eq (1) or (4) and the external disturbance (9) can be represented by a four-dimensional space state. Therefore, it is possible to consider an autonomous dynamical system by introducing a new variable $x_4(t)$. Eqs (1) and (9) can be rewritten as follows:

$$\left.\begin{aligned}
\frac{dC_A}{dt} &= \frac{F_0}{V}(C_{A0} - C_A) - \alpha \cdot C_A \cdot e^{-E/RT} \\
\frac{dT}{dt} &= \frac{F_0}{V}(T_0 + A_t sin(x_4) - T) + \frac{(-\Delta H_R)\alpha}{\rho \cdot c_p} C_A \cdot e^{-E/RT} - \frac{UA}{\rho \cdot c_p V}(T - T_j) \\
\frac{dT_j}{dt} &= \frac{F_j + A_f sin(x_4)}{V_j}(T_{j0} - T_j) + \frac{UA}{\rho_j \cdot c_{pj} V_j}(T - T_j) \\
\frac{dx_4}{dt} &= \omega
\end{aligned}\right\} \qquad (10)$$

Eq (10) represents a four-dimensional model of the reactor with external forcing disturbance, which can be used to investigate the chaotic dynamics.

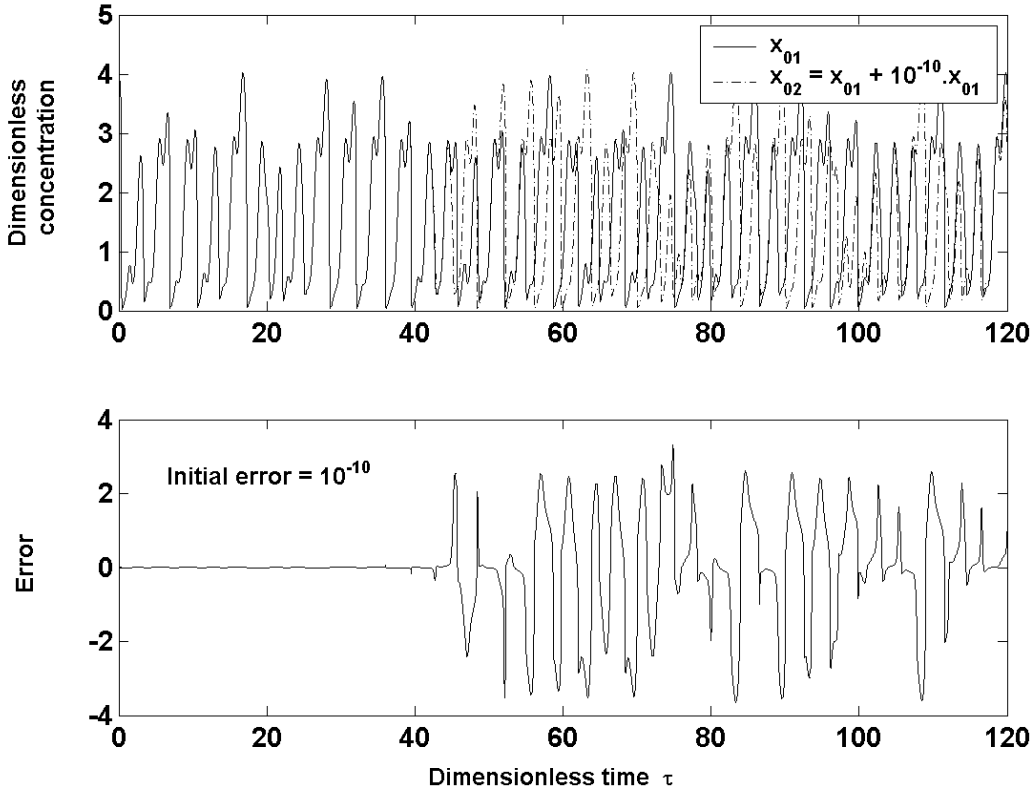

Fig. 4. Sensitivity to initial conditions for the model Eq. (1)-(4) with two very close initial conditions.

The simulation result (Figure 4) shows that when two initial conditions are very close, after a dimensionless time of 40 units the concentration of reactant A and the reactor temperature are completely different. This means that the system has a chaotic behavior and their dynamical states diverge from each other very quickly, i.e. the system has high sensitivity to initial conditions. This separation increases with time and the exponential divergence of adjacent phase points has a very important consequence for the chaotic attractor, i.e. the stretching and folding of the phase space. So, when the reactor reaches chaotic behavior, the trajectories of two adjacent phase points remain bounded

without intersecting, folding themselves, and producing a four-dimensional chaotic attractor with an infinite number of layers. Consequently, the strange attractor of Figure 3 is a projection of the four-dimensional system (10) on the phase plane $C_A(t)$-$T(t)$, and the intersection of trajectories is only apparent. This is in accordance with the fact that phase space trajectories can not intersect themselves.

The reactor has four Lyapunov exponents because the model with the external forcing has four state variables, and their sum should be negative since the system is dissipative. The Lyapunov exponents for the system (10) are shown in Figure 5. Note that one exponent (of variable x_4) corresponds to the direction parallel to the trajectory, so it contributes nothing to the expansion or contraction of the phase volume, and therefore the corresponding Lyapunov exponent is zero. The rest of exponents are negative in the appropriate directions of phase volume, whereas there is one exponent positive, indicating divergence of trajectories. The algorithm used in the calculation of Lyapunov exponents can be found in Benettin, Galgani and Strelcyn, 1980 and it is based on the linearized system trough the trajectory, so it must be combined with the simulation of the nonlinear system (10) (see Appendix).

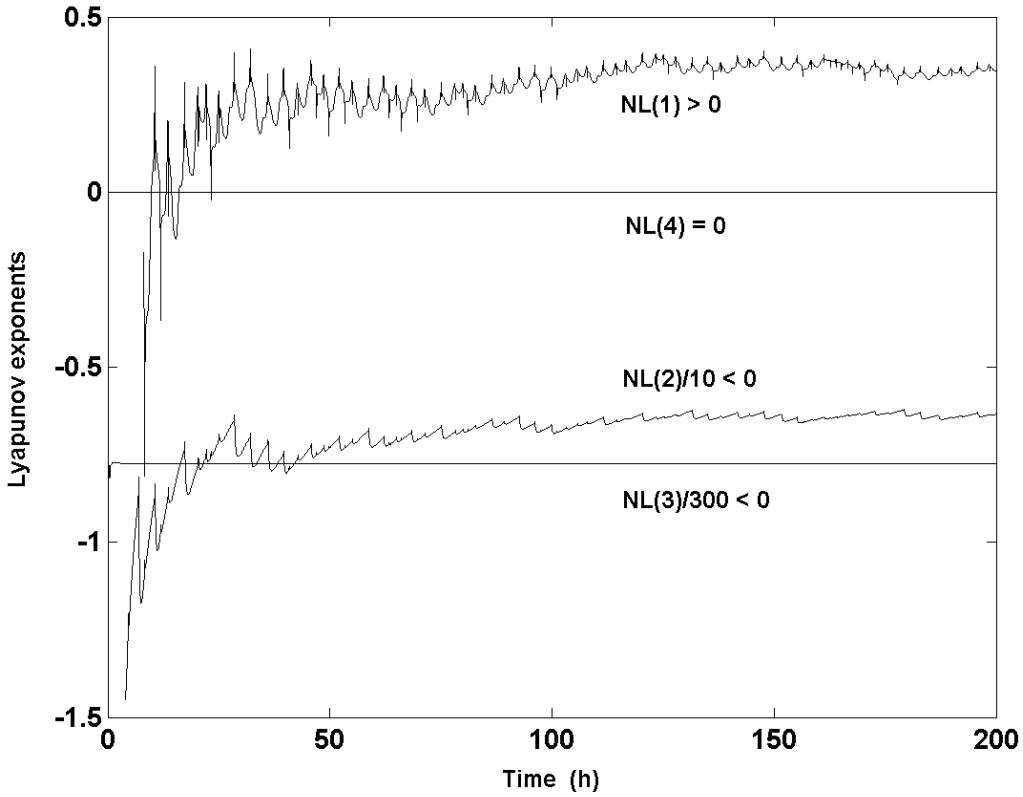

Fig. 5. Lyapunov exponents. C'_{Ao} = 8 kmol/m^3. A_t = 111.1 K; A_f = 0.849 m^3 /h; ω = 5 rad/h

On the other hand, it is well known that there is a relationship between Lyapunov exponents and the divergence of the vector field deduced from the differential equations describing a dynamical system. This relation provides a test on the numerical values developed from the

simulation algorithm. This relationship is, according to the definition of Lyapunov exponents:

$$div\overline{F} = \sum_{i=1}^{4} \lambda_i \;;\; div\overline{F} = \frac{\partial \overline{F}_1(C_A, T, T_j)}{\partial C_A} + \frac{\partial \overline{F}_2(C_A, T, T_j)}{\partial T} + \frac{\partial \overline{F}_3(C_A, T, T_j)}{\partial T_j} \qquad (11)$$

where $div\overline{F}$ means the median value of the divergence of vector field, λ_i is the corresponding Lyapunov exponent and $\overline{F}_1, \overline{F}_2, \overline{F}_3$ are the components of the vector field of Eq (10). The simulation was carried out with fifth order Runge-Kutta-Fehlberg method, with a step interval of T = 0.004 and 0.002 h, and the results are the following:

$$T = 0.004 \Rightarrow div\overline{F} = -241.8684 \;;\; \sum_{i=1}^{4} \lambda_i = -238.4406$$

$$T = 0.002 \Rightarrow div\overline{F} = -241.8267 \;;\; \sum_{i=1}^{4} \lambda_i = -241.9691$$

Consequently, we can ensure that the simulation process is correct. Note that if there is at least one positive Lyapunov exponent, trajectories obtained from two very close initial conditions diverge, and when all Lyapunov exponents are negative the same trajectories converge. A practical procedure to numerically determine the Lyapunov exponents is given in the Appendix.

Exercise 1. From the values of Table 1 and Eq (10), write a computer program using a fourth order Runge-Kutta or fifth order Runge-Kutta-Fehlberg method and reproduce Figures 2,3,4,5. In order to check that the chaotic behavior has been reached, it is necessary to run the program with two initial conditions very close, for example:

$$x_{01} = \left[C_A = 3.93, T = 333.3, T_j = 330.3{,}9, x_4 = 0\right]$$

$$x_{02} = x_{01} + 10^{-10} \cdot x_{01}$$

The dimensionless simulation time must be greater than 100, with a simulation step smaller than 0.004. As the angular variable $x_4(t)$ grows with time, it is convenient to reduce it between 0-2π. The function "atan2(x,y)" is very useful. Note that the chaotic behavior is very sensitive to the parameter values, and can be very interesting to investigate the bifurcation diagram in order to obtain the range of values in the parameter space where the reactor behavior is chaotic. ♦

Figure 6 shows the Fourier power spectrum for the concentration of reactant A (see at Figure 2). Taking into account that the time series at Figure 2 are irregular, the corresponding power spectrum is broadband and contains substantial power at low frequencies. Note that there is a sharp component at the forcing frequency 5 rad/h. It is important to point out that although a positive Lyapunov exponent gives sensitivity to initial conditions it does not guarantee chaotic dynamics. However, in practice, a positive Lyapunov exponent and broad spectrum is sometimes used as an indicator of chaos. The straight line AB has been drawn through the peaks

of the spectrum of frequencies to remark the character of chaotic dynamic, probably due to a route of period-doubling sequences (see Guckenheimer and Holmes, 1983; Wiggins, 1990; Lichtenberg and Lieberman, 1992).

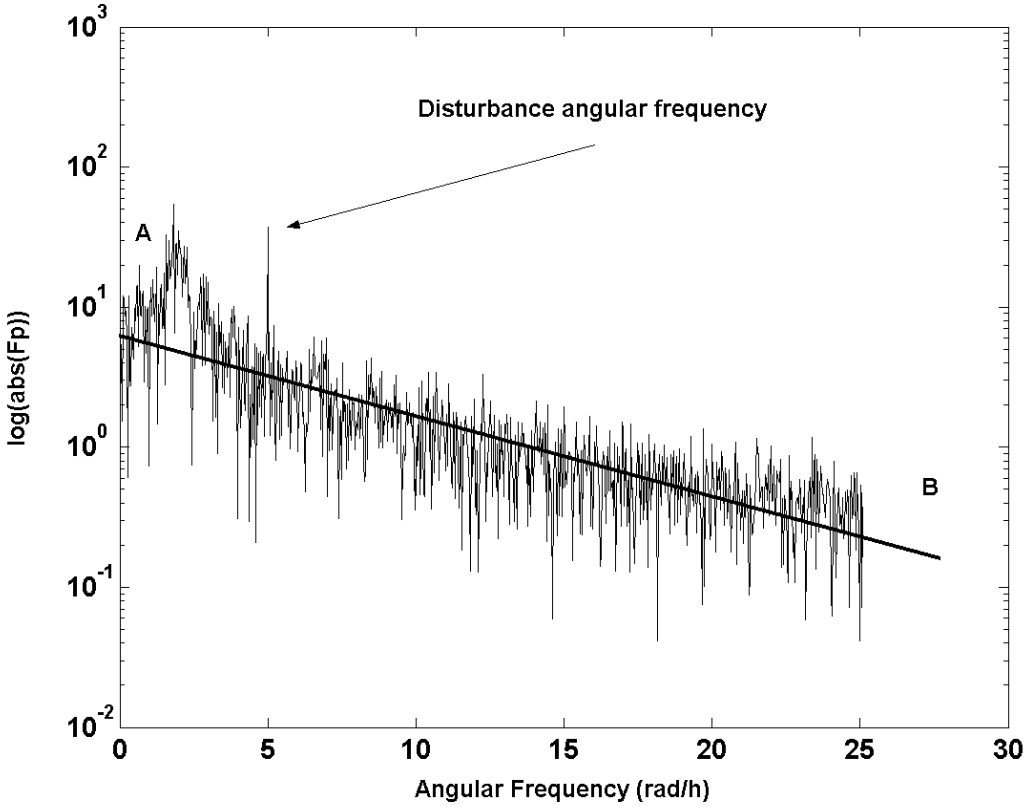

Fig. 6. Power spectrum of reactant concentration A for chaotic behavior. The peak is located at the disturbance angular frequency.

Remark 3. Lyapunov exponents and Fourier analysis have been used as standard criterion for distinguishing between chaotic and non-chaotic dynamics in the past. Nevertheless, these criteria should be interpreted cautiously.

3.2 Self-oscillation and chaotic behavior

A much more interesting case of chaotic dynamics of the reactor can be obtained from the study of the self-oscillating behavior. Consider the simplified mathematical model (8) and suppose that the reactor is in steady state with a reactant concentration of C'_{A0}. The equilibrium point $[x^*, y^*]$ can be deduced as follows:

$$x_0 - x^* - c_0 x^* e^{-1/y^*} = 0 \Rightarrow x^* = \frac{x_0}{1 + c_0 e^{-1/y^*}} \tag{12}$$

$$y_0 - y^* + c_1 x^* e^{-1/y^*} - c_5 (y^* - z_{j0}) = 0 \Rightarrow y_0 = (1 + c_5) y^* - c_5 z_{jo} - \frac{c_1 x_0}{c_0 + e^{1/y^*}} \qquad (13)$$

Eq (13) is transcendent and the variable y^* can not be deduced as a function of the inlet stream dimensionless temperature. Nevertheless it is possible to obtain y_0 as a function of all possible reactor equilibrium temperatures y^*. From Eq (13) it is deduced that:

$$\begin{aligned} &\text{If } y^* \to 0 \Rightarrow y_0 \approx (1 + c_5) y^* - c_5 z_{j0} \\ &\text{if } y^* \to \infty \Rightarrow y_0 \approx (1 + c_5) y^* - \left[c_5 z_{j0} + \frac{c_1 x_0}{c_0 + 1} \right] \end{aligned} \qquad (14)$$

In the plane y_0-y^* Eqs (14) are straight lines of slope $(1+c_5)$, and from intermediate values of y^* it is obtained a curve whose form depends on the value of x_0, as shown in Figure 7.

From Figure 7 it is deduced that the number of the equilibrium states depends on the number of points where the straight line $y_0 = constant$ intersects with the curve defined by Eq (13). With a value of $y_0 \approx 0.025$, there are three equilibrium points P_1, P_2, P_3, being P_1 stable, P_2 unstable and P_3 can be stable or unstable depending on the real part of the eigenvalues of the linearized system at this point. When the line $y_0 = constant$ is tangent to the curve $y_0 = f(y^*)$ (i.e. point M) a new behavior of the reactor appears, which can be characterized from $dy_0/dy^* = 0$ in Eq (13) as follows:

$$\frac{dy_0}{dy^*} = 0 \Rightarrow 1 + c_5 - \frac{c_1 x_0 e^{1/y^*} 1/(y^*)^2}{(c_0 + e^{1/y^*})^2} = 0 \qquad (15)$$

From Eq (15) the value of x_0 can be deduced as a function of the equilibrium value y^*. Substituting this value in Eq (13), the following equations are obtained:

$$\begin{aligned} x_0 &= \frac{1 + c_5}{c_1} (y^*)^2 \left(c_0 + e^{-1/y^*} \right)^2 e^{-1/y^*} \\ y_0 &= (1 + c_5) y^* - c_5 z_{jo} - (1 + c_5)(y^*)^2 \left(1 + c_0 e^{-1/y^*} \right) \end{aligned} \qquad (16)$$

These equations represent a parametric curve with parameter y^*. From a set of values of the parameter y^* it is possible to draw a curve in the x_0-y_0 plane, so we obtain a bifurcation curve as a function of parameter y^*. This curve with a cusp point can be considered as the border that dividing the plane x_0-y_0 into domains with one and three equilibrium states respectively.

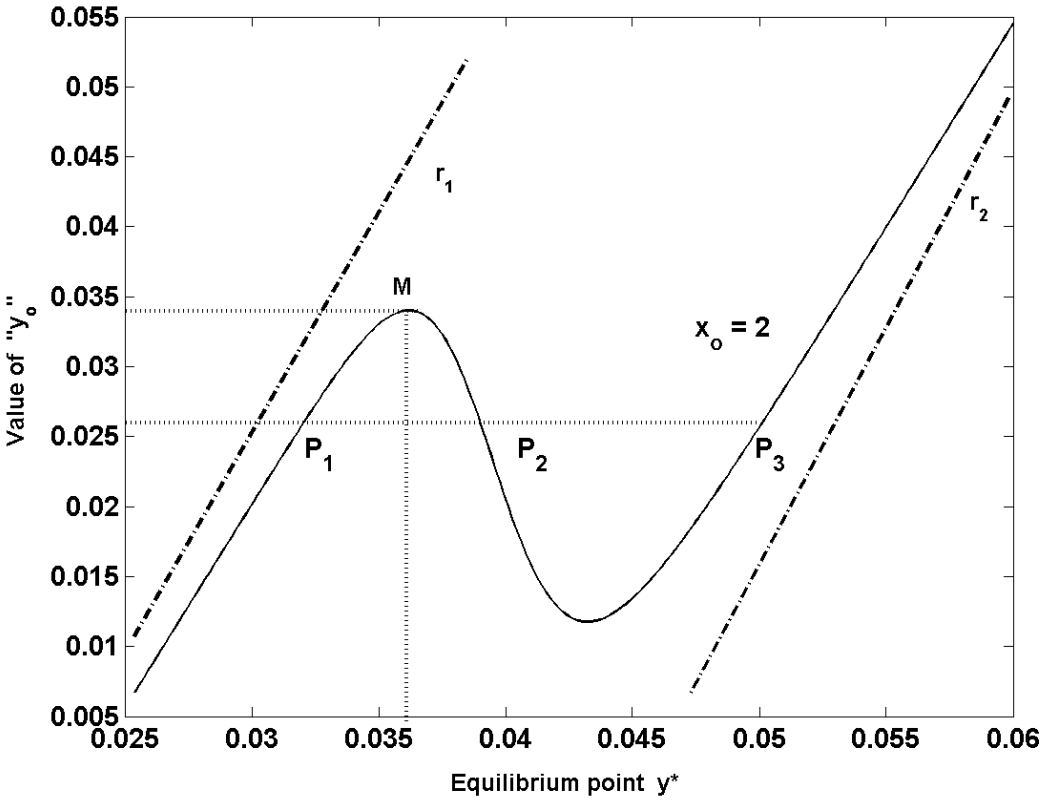

Fig.7. Inlet stream dimensionless temperature vs. equilibrium temperature y^* at a fixed value of the inlet stream dimensionless concentration x_0. The straight-line r_1 and r_2 are defined by Eq (14)

In order to obtain the self-oscillation zone at the plane x_0-y_0 consider the Jacobian of the linearized system (8):

$$J = \begin{bmatrix} a_{11} & a_{12} \\ a_{21} & a_{22} \end{bmatrix} = \begin{bmatrix} -1 - c_0 e^{-1/y^*} & -c_0 \dfrac{x^*}{(y^*)^2} e^{-1/y^*} \\ c_1 e^{-1/y^{**}} & -(1+c_5) + c_1 \dfrac{x^*}{(y^*)^2} e^{-1/y^*} \end{bmatrix} \tag{17}$$

The eigenvalues of matrix (17) depend on the coefficients a_{ij} from the following equation:

$$\lambda^2 - \sigma \cdot \lambda + \Delta = 0 \; ; \; \sigma = -(a_{11} + a_{22}) \; ; \; \Delta = a_{11}a_{22} - a_{12}a_{21} \tag{18}$$

If the following conditions are imposed:

$$\sigma = 0 \; ; \; \Delta > 0 \tag{19}$$

Eq (18) has two complex roots with real part equal to zero, and consequently it is possible to deduce a relation between x^* and y^*.

Substituting in the Eq (12) one obtains a parametric Eq $x_0 = f_1(y^*)$. Eliminating x_0 between $x_0 = f_1(y^*)$ and Eq (13), the parametric equations of self-oscillating behavior are deduced:

$$x_0 = \frac{c_0 (y^*)^2}{c_1}\left[3 + c_5 + \left(\frac{2 + c_5}{c_0}\right)e^{-1/y^*} + c_0 e^{-1/y^{**}}\right] \qquad (20)$$
$$y_0 = (1 + c_5)y^* - c_5 z_{j0} - (y^*)^2\left(2 + c_5 + c_0 e^{-1/y^*}\right)$$

Eqs. (20)define a closed curve or lobe in the plane x_0-y_0. Eqs (16) and (20) are plotted in Figure 8. This Figure shows that when the values of the inlet stream concentration and temperature are inside the dash zone (i.e. inside the lobe and outside the curve with cusp point), the reactor has a self-oscillating behavior. For a point outside the lobe and curve with cusp point, there is only one equilibrium point; this means that the values of inlet stream concentration x_0 and the inlet temperature y_0 give a curve such as the straight line y_0 = constant only intersects the bifurcation curve of Figure 7 at one point. Another interesting consideration is that the lobe is small, and so it can be very difficult to choose values of temperature and concentration of reactant A in the inlet stream to the reactor to get an oscillating regime. If the reactor is being forced with an external periodic disturbance, and the values of x_0 , y_0 are inside the lobe, it is possible that the reactor reaches the chaotic behavior.

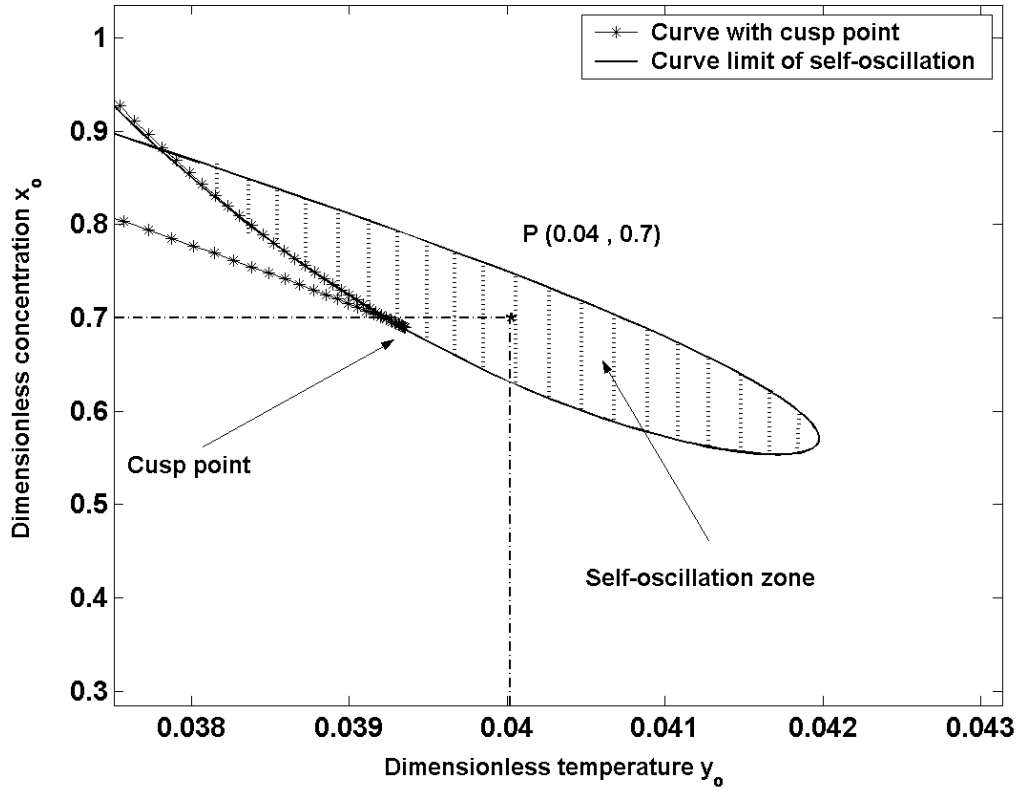

Fig. 8. Self-oscillating and three-equilibrium state regions for a CSTR

Figure 8 shows a point P inside the lobe, and Figure 9 shows the simulation results when the inlet stream concentration and temperature are inside the lobe: a trajectory approaches a closed curve or limit cycle and remains there. This behavior has been corroborated in an industrial environment

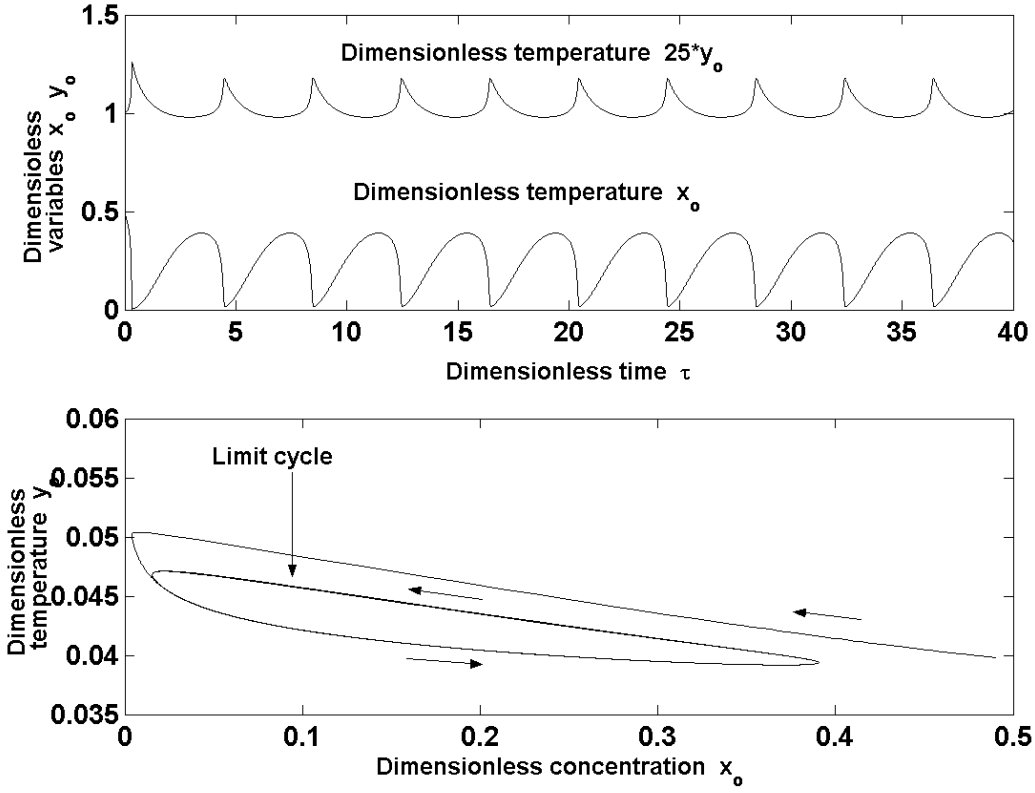

Fig. 9. Self-oscillating behavior with values $x_0 = 0.7$ and $y_0 = 0.04$ inside the lobe

Exercise 2. Using the values from Table 1 and the Eq (5), (13) write a computer program to obtain Figure 7 from different values of x_o and check the Eq (14). From different values of equilibrium point (x^*,y^*) determine the curve with cusp point and the lobe of Figure 8. These curves can be difficult to visualize if the values of (x^*,y^*) are not appropriate. In order to do it choose values of y^* between the maximum and minimum of the curve at Figure 7. Why? Using the program of exercise 1 and taking $A_t = 0$, $A_f = 0$ and a point (x_o,y_o) inside the lobe check the self-oscillating behavior shown at Figure 9. Make a zoom at Figure 8 to obtain a pair of values (x_o,y_o) inside the zone of curve with cusp point and curve limit of self-oscillation. Can we obtain self-oscillation behavior? Why?. ♦

Exercise 3. From the simulation program of exercise 1 or 2 determine the power spectrum of Figure 6. One easy way is the following. From the simulation program one obtains the values of x(t), y(t) and z(t), so the fast Fourier transform can be calculated from a standard commercial program such as Maple, Mathematica, Matlab etc. Only the half components of positive frequency must be considered. The absolute values of these

components using semilog coordinates give us the power spectra of Figure 6.♦

Another interesting aspect of the self-oscillating behavior is the following. If the values of (x_o, y_o) are inside the lobe, an external periodic disturbance of the coolant flow rate can drive the reactor to chaotic behavior.

It is important to remark that this behavior is similar to that previously considered by Eq (9), when two external periodic disturbances are applied. Nevertheless, this behavior can be very difficult to obtain, because the lobe of Figure 8 is small. Figures 10 and 11 shows chaotic oscillations and a new strange attractor. By simulation it is possible to obtain plots similar to those in Figures 2,4,5 and 6.

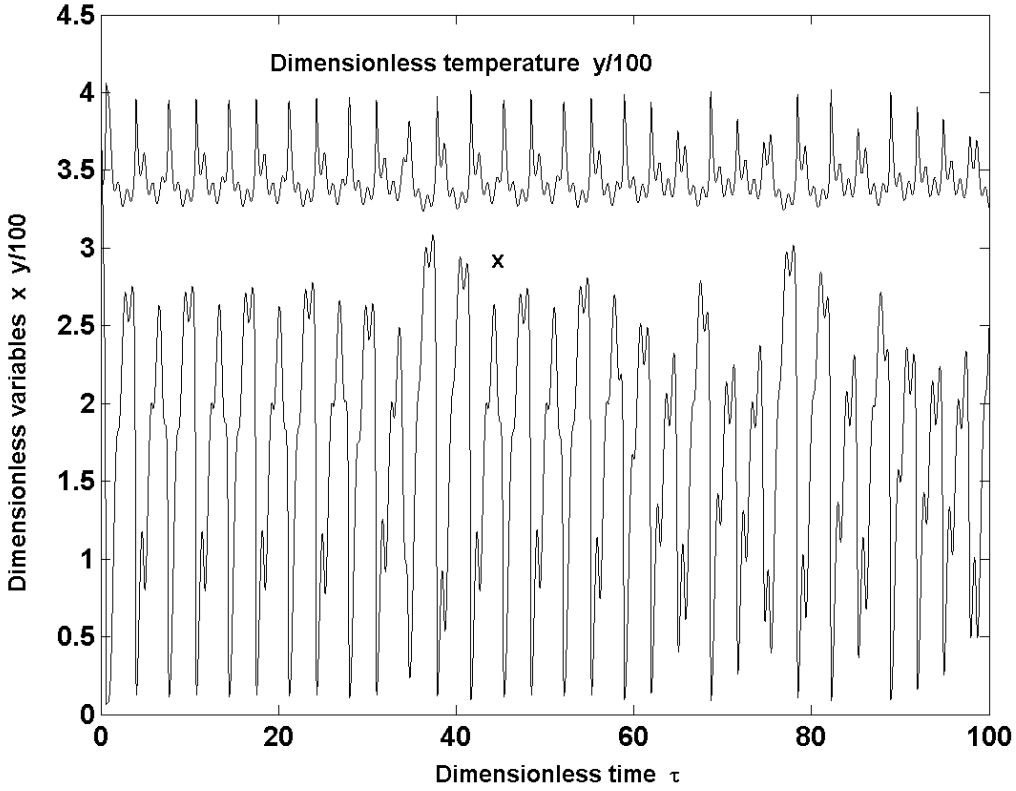

Figure 10. Chaotic oscillations for the two-dimensional model (8). $A_t = 0$; $A_f = 0.849\ m^3/h$; $\omega = 6.5$

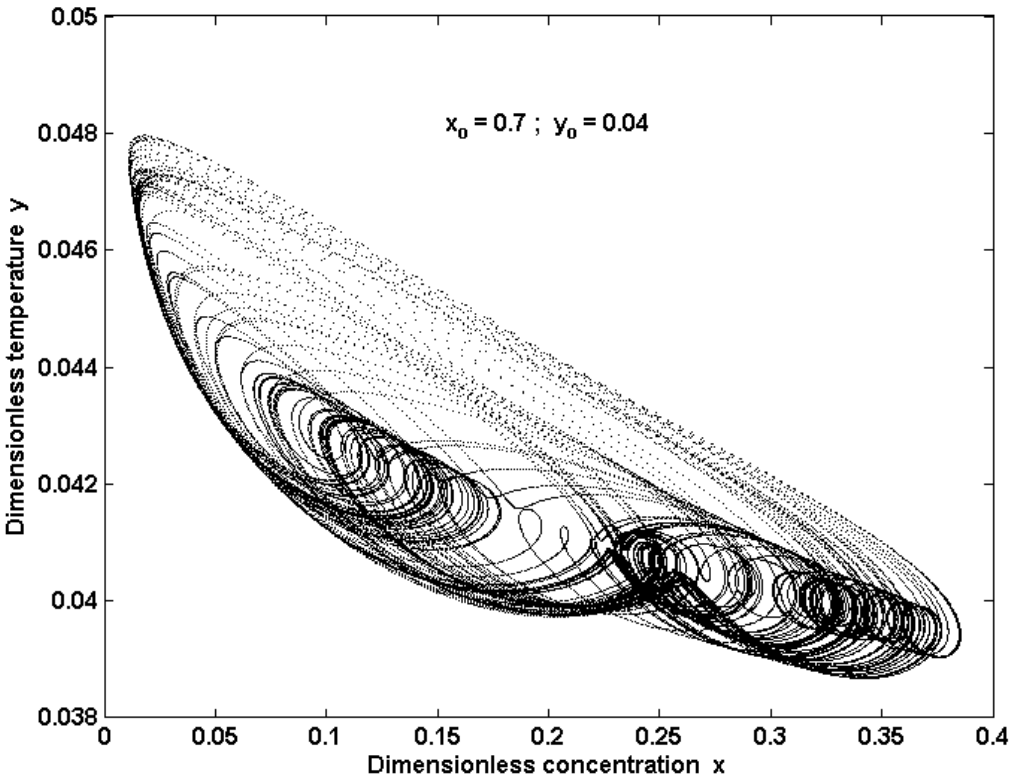

Figure 11. Strange attractor for the model (8). C'_{Ao} = 8 kmol/m^3

4 Regular self-oscillation and chaotic behavior of a CSTR with PI control

In this section we consider a CSTR with a very simple control system formed by two PI controllers. The first controller manipulates the outlet flow rate as a function of the volume in the tank reactor. A second PI controller manipulates the flow rate of cooling water to the jacket as a function of error in reactor's temperature. The control scheme is shown in Figure 12 where the manipulated variables are the inlet coolant flow rate F_j and the outlet flow rate F respectively.

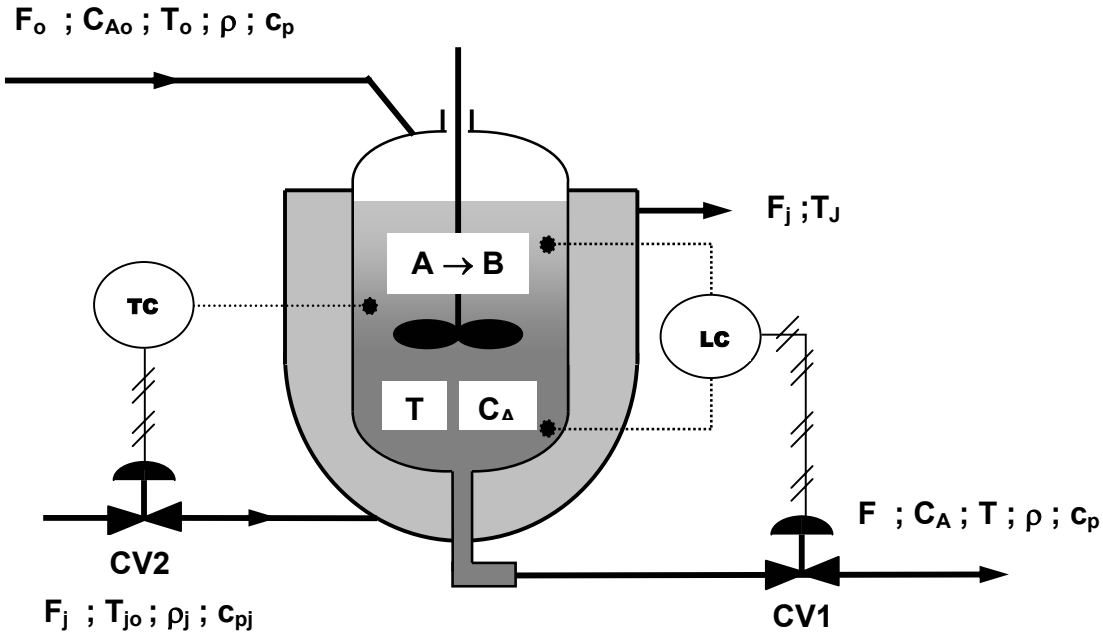

Figure 12. Perfectly mixed CSTR with two PI controllers.

Considering the assuptions taken in section 2, the modelling equations of the reactor with two PI controllers are the following:

$$\left.\begin{aligned}
&\frac{dV}{dt} = F - F_0 \\
&\frac{dC_A}{dt} = \frac{F_0}{V}(C_{A0} - C_A) - \alpha \cdot C_A \cdot e^{-E/RT} \\
&\frac{dT}{dt} = \frac{F_0}{V}(T_0 - T) + \frac{(-\Delta H_R)\alpha}{\rho \cdot c_p} C_A \cdot e^{-E/RT} - \frac{UA}{\rho \cdot c_p V}(T - T_j) \\
&\frac{dT_j}{dt} = \frac{F_j}{V_j}(T_{j0} - T_j) + \frac{UA}{\rho_j \cdot c_{pj} V_j}(T - T_j) \\
&\frac{dF}{dt} = K_v \frac{dV}{dt} + \frac{K_v}{t_1}(V - V_s) \\
&\frac{dF_j}{dt} = K_t \frac{dT}{dt} + \frac{K_t}{t_2}(T - T_{set})
\end{aligned}\right\} \qquad (21)$$

where the volume of liquid in the reactor must be considered as variable and the last two equations of (21) represent the equations of the PI controllers. The variables V_s and T_{set} are the steady state volume and set point temperature of the reactor respectively, and K_v, t_1 and K_t, t_2 are the constant of proportional and integral action of each one of the PI controllers. We assume that the manipulated variable F_j is constrained due to saturation of the control valve CV2:

$$0 \le F_j \le F_{jmax} \tag{22}$$

where F_{jmax} is the maximum value of cooling water through the control valve CV2. The outlet flow through the control valve CV1 is not limited because it is assumed that its size exceeds the nominal one. The variables F_0, C_{A0}, T_0, T_{j0} can be considered as external load disturbances whose effect must be minimized by the PI controllers. Equation (21) and (22) can be difficult to analyze. So, similarly to section 2, in order to simplify the mathematical treatment, it is useful to introduce dimensionless variables as follows:

$$\tau = \frac{F_{0s}t}{V_s} \; ; \; x_1 = \frac{V}{V_s} \; ; \; x_5 = \frac{F}{F_{0s}} \; ; \; x_{50} = \frac{F_0}{F_{0s}} \; ; \; x_2 = \frac{C_A}{C'_{A0}} \; ; \; x_{20} = \frac{C_{A0}}{C'_{A0}} \tag{23}$$

$$\frac{1}{x_3} = \frac{E}{RT} \; ; \; \frac{1}{x_{30}} = \frac{E}{RT_0} \; ; \; \frac{1}{x_4} = \frac{E}{RT_j} \; ; \; \frac{1}{x_{40}} = \frac{E}{RT_{j0}} \; ; \; \frac{1}{x_s} = \frac{E}{RT_{set}} \; ; \; x_6 = \frac{F_j}{F_{js}} \; ; \; x_{6max} = \frac{F_{jmax}}{F_{js}} \tag{24}$$

where F_{0s} is the steady state inlet flow rate, C'_{A0} is the initial concentration of the reactant A in the reactor and F_{js} is the steady state of the coolant flow rate. The dimensionless constants of the PI controllers are the following:

$$K_{vd} = K_v \frac{V_s}{F_{0s}} \; ; \; \tau_{1d} = t_1 \frac{F_{0s}}{V_s} \; ; \; K_{td} = K_t \frac{T_0}{F_{js}} \; ; \; \tau_{2d} = t_2 \frac{F_{0s}}{V_s} \tag{25}$$

Introducing the parameters:

$$\begin{gathered} c_0 = \frac{V_s}{F_{0s}}\alpha \; ; \; c_1 = \frac{V_s R(-\Delta H_R)C'_{A0}}{F_{0s}E\rho \cdot c_p}\alpha \; ; \; c_2 = \frac{UA}{\rho \cdot c_p F_{0s}} \\ c_3 = \frac{V_s F_{js}}{V_j F_{0s}} \; ; \; c_4 = \frac{\rho \cdot c_p V_s}{\rho_j c_{pj} V_j} c_2 \end{gathered} \tag{26}$$

the equations of the reactor in dimensionless variables can be written as:

$$\left.\begin{aligned} \frac{dx_1}{d\tau} &= x_{50} - x_5 \\ \frac{dx_2}{d\tau} &= \frac{x_{50}}{x_1}(x_{20} - x_2) - c_0 \cdot x_2 \cdot e^{-1/x_3} \\ \frac{dx_3}{d\tau} &= \frac{x_{50}}{x_1}(x_{30} - x_3) + c_1 \cdot x_2 \cdot e^{-1/x_3} - \frac{c_2}{x_1}(x_3 - x_4) \\ \frac{dx_4}{d\tau} &= c_3 \cdot x_6 \cdot (x_{40} - x_4) + c_4 \cdot (x_3 - x_4) \\ \frac{dx_5}{d\tau} &= K_{vd}(x_{50} - x_5) + \frac{K_{vd}}{\tau_{1d}}(x_1 - 1) \\ \frac{dx_6}{d\tau} &= \frac{K_{td}}{x_{30}}\frac{dx_3}{d\tau} + \frac{K_{dt}}{x_{30}\tau_{2d}}(x_3 - x_s) \\ 0 &\le x_6 \le x_{6\max} \end{aligned}\right\} \tag{27}$$

where only the sate variable x_6 is bounded.

From Eq (27) it is possible to determine the equilibrium points following a similar procedure to section 3.1, consequently Figures as 7, 8 can be obtained.

Exercise 4. From Eqs (27) prove that the dimensionless coolant temperature can be written as:

$$x_{4e} = \left(\frac{x_{50} + c_2}{c_2} \right) \cdot x_s - \frac{x_{30} \cdot x_{50}}{c_2} - \frac{c_1}{c_2} \frac{x_{20} \cdot x_{50}}{x_{50} \cdot e^{1/x_s} + c_0} \tag{28}$$

For different values of x_s draw the function $x_{4e} = f(x_s)$ taking x_{20} as parameter. Show the possibility to obtain one, two or three equilibrium points. Prove that the following inequality is verified:

$$x_{4emin} \le \frac{x_s + x_{6max} \cdot x_{40} \cdot (c_3 / c_4)}{1 + x_{6max} \cdot (c_3 / c_4)} \le x_s \tag{29}$$

From different values of x_{20} and by using the values from table 1 write a computer program to obtain a figure similar to Figure 7. ♦

Exercise 5. Taking into account exercise 4 prove that the parametric equations of curve with cusp point are the following:

$$\begin{aligned} x_{20} &= \left(\frac{x_{50} + c_2}{c_1} \right) \cdot x_s^2 \cdot e^{-1/x_s} \cdot (c_0 + e^{1/x_s})^2 \\ x_{30} &= (x_{50} + c_2) \cdot x_s - c_2 \cdot x_{4e} - (x_{50} + c_2) \cdot x_s^2 \cdot (1 + c_0 \cdot e^{-1/x_s}) \end{aligned} \tag{30}$$

♦

Eqs. (27) can be simplified taking into account that the first and fifth equations are independent, so eliminating the x_5 variable the following linear differential equation is obtained:

$$\frac{d^2 x_1}{d\tau^2} + K_{vd} \frac{dx_1}{d\tau} + \frac{K_{vd}}{\tau_{1d}} x_1 = \frac{K_{vd}}{\tau_{1d}} \; ; \; x_1(0) = 1 \; ; \left(\frac{dx_1(\tau)}{d\tau} \right)_{\tau=0} = x_{50} - 1 \tag{31}$$

Note that there is no interaction between the volume of the reactor and its temperature.

Eq (31) can be used to adjust the parameter of the PI controller LC at Figure 12. For example, complex roots of the characteristic equation of (30) gives the following dimensionless volume of the reactor:

$$x_1(\tau) = 1 + \frac{x_{50} - 1}{\sqrt{\frac{K_{vd}}{\tau_{1d}} \cdot \sqrt{1 - \frac{\tau_{1d} K_{vd}}{4}}}} \cdot e^{-\frac{K_{vd}}{2}\tau} \cdot sin\left\{ \sqrt{\frac{K_{vd}}{\tau_{1d}}} \sqrt{1 - \frac{\tau_{1d} K_{vd}}{4}} \cdot \tau \right\} \tag{32}$$

Eq (32) can be written as:

$$x_1(\tau) = 1 + f(\tau)\ ;\ f(\tau) = \frac{x_{50} - 1}{\sqrt{\frac{K_{vd}}{\tau_{1d}} \cdot \sqrt{1 - \frac{\tau_{1d} K_{vd}}{4}}}} \cdot e^{-\frac{K_{vd}}{2}\tau} \cdot sin\left\{ \sqrt{\frac{K_{vd}}{\tau_{1d}}} \sqrt{1 - \frac{\tau_{1d} K_{vd}}{4}} \cdot \tau \right\} \qquad (33)$$

Substituting Eq (33) into Eqs. (27) the dimensionless equations of the reactor are simplified as follows:

$$\left.\begin{aligned}
\frac{dx_2}{d\tau} &= x_{50}(x_{20} - x_2) - c_0 \cdot x_2 \cdot e^{-1/x_3} - \frac{x_{50} f(\tau)}{1 + f(\tau)} \cdot (x_{20} - x_2) \\
\frac{dx_3}{d\tau} &= x_{50}(x_{30} - x_3) + c_1 \cdot x_2 \cdot e^{-1/x_3} - c_2(x_3 - x_4) - \frac{f(\tau)}{1 + f(\tau)} \cdot \left[x_{50}(x_{30} - x_3) - c_2(x_3 - x_4) \right] \\
\frac{dx_4}{d\tau} &= c_3 x_6 \cdot (x_{40} - x_4) + c_4 \cdot (x_3 - x_4) \\
\frac{dx_6}{d\tau} &= \frac{K_{td}}{x_{30}} \cdot \frac{dx_3}{d\tau} + \frac{K_{td}}{x_{30}\tau_{2d}} \cdot (x_3 - x_s)
\end{aligned}\right\} \qquad (34)$$

Eqs. (34) are a set of differential equations, which lead a flow in a four dimensional phase space R^4. This flow can be simplified to three dimensional phase space R^3 when the dynamics of the jacket can be considered negligible respect to the reactor's dynamics. Putting $dx_4/d\tau = 0$ the dimensionless jacket's temperature x_4 can be eliminated from Eqs. (34), and the simplified mathematical model of the reactor can be written as

$$\left.\begin{aligned}
\frac{dx_2}{d\tau} &= x_{50}(x_{20} - x_2) - c_0 \cdot x_2 \cdot e^{-1/x_3} - \frac{x_{50} f(\tau)}{1 + f(\tau)} \cdot (x_{20} - x_2) \\
\frac{dx_3}{d\tau} &= x_{50}(x_{30} - x_3) + c_1 \cdot x_2 \cdot e^{-1/x_3} - \frac{c_2 c_3 x_6 (x_3 - x_{40})}{c_3 x_6 + c_4} - \frac{f(\tau)}{1 + f(\tau)} \cdot \left[x_{50}(x_{30} - x_3) - \frac{c_2 c_3 x_6 (x_3 - x_{40})}{c_3 x_6 + c_4} \right] \\
\frac{dx_6}{d\tau} &= \frac{K_{td}}{x_{30}} \cdot \frac{dx_3}{d\tau} + \frac{K_{td}}{x_{30}\tau_{2d}} \cdot (x_3 - x_s)
\end{aligned}\right\} \qquad (35)$$

Note that from Eq (33) the function f (τ) = 0 if there is not disturbance in the inlet flow to the reactor *($x_{50} = 1$)* and consequently, the equilibrium point of the reactor can be obtained from the following equations:

$$\left.\begin{aligned}
\frac{dx_2}{d\tau} &= f_1(x_2, x_3, x_6) = x_{50}(x_{20} - x_2) - c_0 \cdot x_2 \cdot e^{-1/x_3} \\
\frac{dx_3}{d\tau} &= f_2(x_2, x_3, x_6) = x_{50}(x_{30} - x_3) + c_1 \cdot x_2 \cdot e^{-1/x_3} - \frac{c_2 c_3 x_6 (x_3 - x_{40})}{c_3 x_6 + c_4} \\
\frac{dx_6}{d\tau} &= f_3(x_2, x_3, x_6) = \frac{K_{td}}{x_{30}} \cdot \left[x_{50}(x_{30} - x_3) + c_1 \cdot x_2 \cdot e^{-1/x_3} - \frac{c_2 c_3 x_6 (x_3 - x_{40})}{c_3 x_6 + c_4} \right] + \frac{K_{td}}{x_{30}\tau_{2d}} \cdot (x_3 - x_s)
\end{aligned}\right\} \qquad (36)$$

The same Eqs. (36) can be approximately considered when the dimensionless time τ is as high as consider the exponential factor of $f(\tau)$ in Eq (33) negligible.

Exercise 6. Show that the equilibrium point of the model R^4 defined by Eqs. (34) and the simplified model R^3 given by Eqs. (34), i.e. when the dynamics of the jacket is considered negligible, are the same. Deduce the jacobian of the system (35) at the corresponding equilibrium point. Write a computer program to determine the eigenvalues of the linearized model R^3 at the equilibrium point as a function of the dimensionless inlet flow x_{50}. Values of the dimensionless parameters of the PI controller can be fixed at K_{td} = 1.52 ; τ_{2d} = 5. The set point dimensionless temperature and the inlet coolant flow rate temperature are x_s = 0.0398, x_{40} = 0.0351 respectively. An appropriate value of dimensionless reference concentration is C'_{A0} = 0.245. Does it exist some value of x_{50} for which the eigenvalues of the linearized system R^3 at the equilibrium point are complex with zero real part? Note that it is necessary to vary x_{50} from small to great values. Check the possibility to obtain similar results for the R^4 model.♦

It is interesting to point out that the regular behavior, where a steady state is reached by the reactor, can be investigated from the models defined by Eqs. (33) or (34), taking into account different values of the PI controllers. The values of K_{vd} and τ_{1d} are chosen from the inequality:

$$\left(\frac{K_{vd}}{2}\right)^2 < \frac{K_{vd}}{\tau_{1d}} \tag{37}$$

The values of K_{td} and τ_{2d} from Eq.(36) can be obtained from the transfer function of the linearized model at the equilibrium point, applying conventional methods from the linear control theory (See part 1). In order to investigate the self-oscillating behavior, one can determine the linearized system at the equilibrium point, and the corresponding complex eigenvalues with zero real part, when the parameters K_{td} and τ_{2d} of the PI controller are varied. For example, taking into account Eqs. (34), the jacobian matrix of the linearized system at dimensionless set point temperature x_s is the following:

$$\mathbf{J} = \begin{bmatrix} -x_{50} - c_0 e^{-1x_s} & -c_0 \dfrac{x_{2e}}{x_s^2} e^{-1/x_s} & 0 & 0 \\ c_1 e^{-1/x_s} & -(x_{50}+c_2) + c_1 \dfrac{x_{2e}}{x_s^2} e^{-1/x_s} & c_2 & 0 \\ 0 & c_4 & -(c_3 x_{6e} + c_4) & c_3(x_{40} - x_{4e}) \\ \dfrac{K_{td}}{x_{30}} c_1 e^{-1/x_s} & \dfrac{K_{td}}{x_{30}}\left[-(x_{50}+c_2) + c_1 \dfrac{x_{2e}}{x_s^2} e^{-1/x_s}\right] + \dfrac{K_{td}}{x_{30}\tau_{2d}} & \dfrac{K_{td}}{x_{30}} c_2 & 0 \end{bmatrix} \tag{38}$$

and the characteristic equation of can be written as:

$$\left|\lambda \cdot \mathbf{I} - \mathbf{J}\right| = \lambda^4 + S_1\lambda^3 + S_2\lambda^2 + S_3\lambda + S_4 \;;\; S_i = (-1)^i \sum \left|A_{i_k}^{i_k}\right| \tag{39}$$

where S_i are the sum of the principal minors of $\mathbf{J}$. Taking into account the Routh stability criterion, the Routh array is formed as given below:

$$\begin{array}{|cc} 1 & S_2 \quad S_4 \\ S_1 & S_3 \\ (S_1S_2 - S_3)/S_1 & S_4 \\ \dfrac{(S_1S_2S_3 - S_3^2)/S_1 - S_1S_4}{(S_1S_2 - S_3)/S_1} & \\ S_4 & \end{array}$$

Assuming that $S_1 > 0$, $S_4 > 0$ and $S_1 S_2 - S_3 > 0$, the condition of self-oscillating behavior is given by the equation:

$$S_1S_2S_3 - S_3^2 - S_1^2S_4 = 0 \tag{40}$$

and the frequency of self-oscillations is:

$$\omega = \sqrt{\frac{S_1S_4}{S_1S_2 - S_3}} \tag{41}$$

Figure 13 shows the variation of K_{td} for various values of τ_{2d} and the corresponding frequencies of self-oscillation. Figure 14 shows the oscillation behavior of the reactor with the value $x_s = 0.0398$ and $\tau_{2d} = 0.5$, Ktd = 19.6.

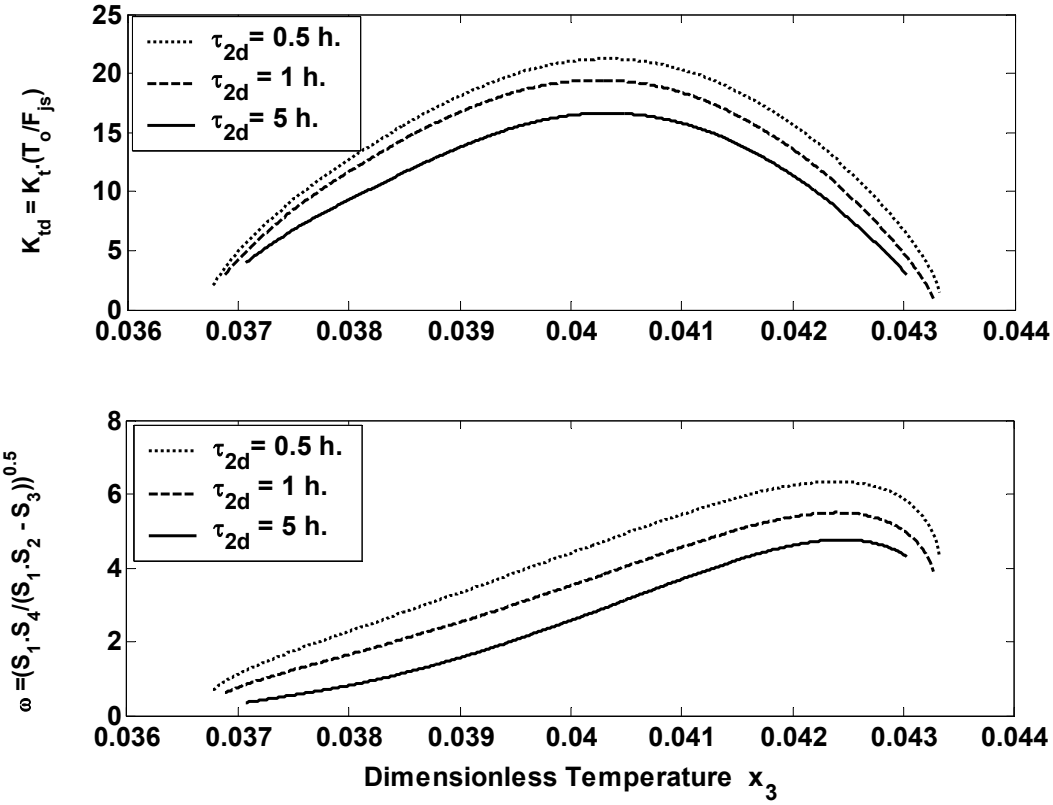

Figure 13. Dimensionless constant K_{td} and self-oscillating frequency for different constant integral action τ_{2d}

Note that Figure 13 can be used to compare the parameters of the controller when they are obtained from the Ziegler-Nichols or Cohen-Coom rules. On the other hand, at Figure 14 it can be observed that the outlet dimensionless flow rate and the reactor volume reaches the steady state whereas the dimensionless reactor temperature remain in self-oscillation regime. The knowledge of the self-oscillation regime in a CSTR is important, both from theoretical and experimental point of view, because there is experimental evidence that the self-oscillation behavior can be useful in an industrial environment.

In Eqs (33), (34) and (35) the effect of the constrained coolant flow rate due to control valve saturation is not considered, however this limitation can be introduced in the mathematical model of the reactor as follows:

$$sat(x_6) = \begin{cases} 0 & \text{for} \quad x_6 \le 0 \\ x_6 & \text{for} \quad 0 \le x_6 \le x_{6max} \\ x_{6max} & \text{for} \quad x_6 > x_{6max} \end{cases} \tag{42}$$

The model R^3 of the reactor can be written as:

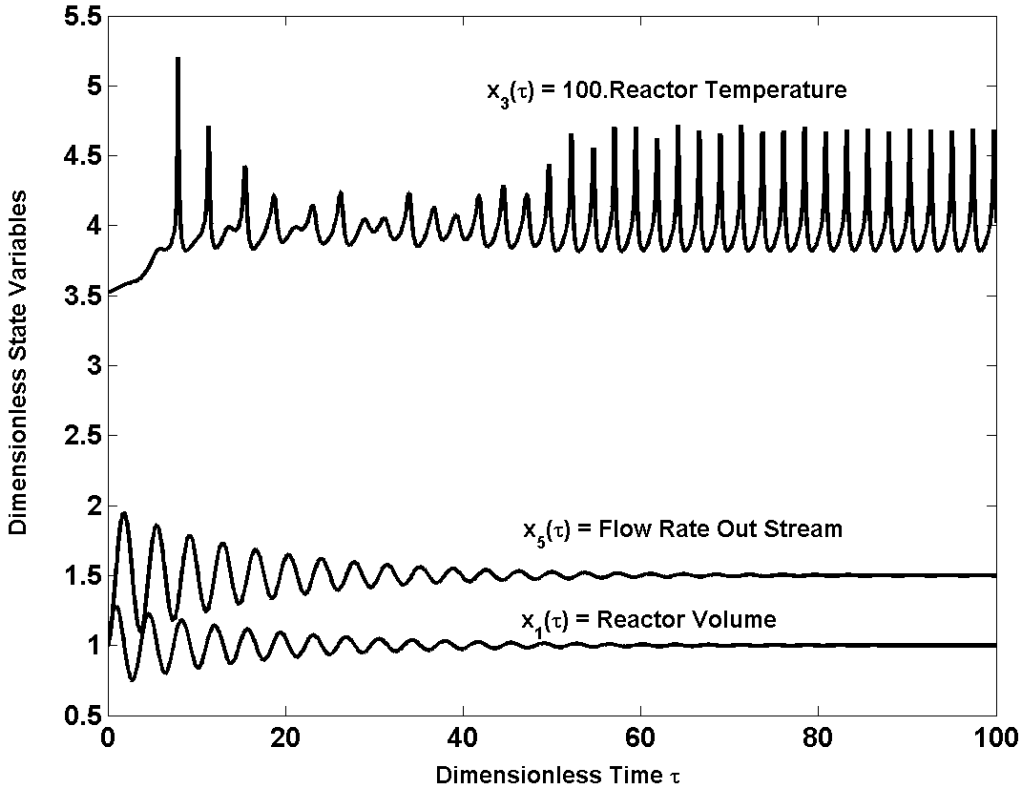

Figure 14. Self-oscillation behavior with K_{td} = 19.6; τ_{2d} = 0.5

$$\left.\begin{aligned}
\frac{dx_2}{d\tau} &= x_{50}(x_{20}-x_2)-c_0\cdot x_2\cdot e^{-1/x_3}-\frac{x_{50}f(\tau)}{1+f(\tau)}\cdot(x_{20}-x_2)\\
\frac{dx_3}{d\tau} &= x_{50}(x_{30}-x_3)+c_1\cdot x_2\cdot e^{-1/x_3}-\frac{c_2c_3sat(x_6)(x_3-x_{40})}{c_3sat(x_6)+c_4}-\frac{f(\tau)}{1+f(\tau)}\cdot\left[x_{50}(x_{30}-x_3)-\frac{c_2c_3sat(x_6)(x_3-x_{40})}{c_3sat(x_6)+c_4}\right]\\
\frac{dx_6}{d\tau} &= \frac{K_{td}}{x_{30}}\cdot\frac{dx_3}{d\tau}+\frac{K_{td}}{x_{30}\tau_{2d}}\cdot(x_3-x_s)
\end{aligned}\right\} \tag{43}$$

Eq (42) and (43) will be used in the analysis of the chaotic behavior.

4.1. Analysis of the constrained coolant flow rate

Consider the model's reactor assuming saturation in the control valve and negligible dynamic's jacket as shows in Eqs. (43). The steady states of system (43) can be obtained considering that the derivatives of the left hand of Eqs. (43) are nil and

$$\lim_{\tau\to\infty} f(\tau)=0 \tag{44}$$

However, due to limitation in x_6 dimensionless flow rate of cooling water it is necessary to consider two cases, depending on wherever x_6 is or constrained or limited by the maximum opening of the control valve.

4.1.1. The fluid flow through the control valve is not limited.

This means that the value of the flow rate cooling water is enough to cool down the reactor and consequently, the reactor temperature can reach the desired set point. Therefore, the coolant flow rate reaches a certain steady state value x_{6e}, then from the third of Eqs. (43) it can be deduced that:

$$\left(\frac{dx_6}{d\tau}\right)_{equilibrium}=\frac{K_{td}}{x_{30}}\cdot\left(\frac{dx_3}{d\tau}\right)_{equilibrium}+\frac{K_{td}}{x_{30}\cdot\tau_{2d}}\cdot(x_{3e}-x_s) \tag{45}$$

where x_{3e} is the equilibrium dimensionless temperature of the reactor. Taking into account that in equilibrium the derivatives of Eq (45) are nil, it is deduced that the equilibrium dimensionless reactor temperature must be equal to dimensionless set point temperature $x_{3e} = x_s$, thus the control system drives the reactor to the desired set point.

From Eqs. (43) and (44), and considering the derivatives of the left-hand side to be zero, the values of dimensionless variables in steady state are the following:

$$x_{2e}=\frac{x_{50}x_{20}}{x_{50}+c_0e^{-1/x_s}} \tag{46}$$

$$x_{6e}=\frac{c_4\cdot\left[x_{50}(x_{30}-x_s)+c_1x_{2e}e^{-1/x_s}\right]}{c_2c_3(x_s-x_{40})-c_3x_{50}(x_{30}-x_s)-c_1c_3x_{2e}e^{-1/x_s}} \tag{47}$$

where the values of x_{2e} and x_{6e} are the values of steady state. The equilibrium dimensionless jacket's temperature is calculated from the equation:

$$x_{4e} = \frac{c_1 x_{6e} x_{40} + c_4 x_s}{c_3 x_{6e} + c_4} \tag{48}$$

4.1.2. The dimensionless cooling flow is constrained

In this case it is not possible to reach any value of equilibrium dimensionless coolant flow rate x_{6e}, because when x_{6e} is greater than x_{6max}, it is constrained to the maximum value x_{6max} due to the flow rate limitation through the control valve. From this moment, the derivative $(dx_6/d\tau)$ is zero and the flow rate cooling x_6 remains constant. Consequently, the coolant flow rate cannot decrease the reactor temperature, which reaches a value greater than the set point, and the corresponding reactant concentration will be smaller. From Eqs.(43) the set point temperature must be equal to x_{3e}, and as a result it is impossible that the reactor temperature would be able to reach the set point temperature x_s, an consequently the control system cannot drive the reactor to the desired equilibrium point. The equilibrium values of dimensionless variables are given by the same Eqs (45), (46) and (47), but making the substitutions:

$$x_{6e} = x_{6max} \quad ; \quad x_s = x_{3e} \tag{49}$$

Substituting Eq (49) into Eqs. (43), it can be deduced that

$$\frac{c_2 c_3 x_{6max}}{c_3 x_{6max} + c_4} = \frac{x_{50}(x_{30} - x_{3e})}{x_{3e} - x_{40}} + \frac{x_{50} x_{20} c_1}{(x_{3e} - x_{40}) \cdot (c_0 + x_{50} e^{-1/x_{3e}})} \tag{50}$$

Eq (50) shows the variation of the equilibrium dimensionless temperature as a function of the maximum value of the dimensionless coolant flow rate x_{6max}. Plotting x_{6max} versus x_{3e} a bifurcation curve can be obtained, from which it is possible to determine the value of x_{6max} which gives a different behavior of the reactor in steady state. It is interesting to note that Eq (50) is equal to Eq (47) when we make the substitutions of Eq (49) into Eq (47). However, these equations are conceptually different because from a practical viewpoint, the value of x_s is limited to a small value, while x_{3e} is not.

The curve of maximum dimensionless cooling temperature x_{6max} versus the equilibrium dimensionless reactor temperature from Eq (50) is shown in Figure 15. This plot shows the possibility of three steady state states corresponding to the same value of x_{6max}. The three steady sates are the points of intersection P_1, P_2 and P_3 of plot with the horizontal line corresponding to a value of x_{6max}. Once the steady state has been found, it is necessary to know how stable they are. Let's assume that in equilibrium the reactor is at point P'_2. At this point the equilibrium temperature is greater than point P_2. This will cause the maximum dimensionless coolant flow rate x_{6max} inlet reactor' jacket to raise, and the raising will continue until the upper maximum point M. It is easy to show, using similar arguments that P_1 and P_3 are steady state and P_2 is an unstable one.

However, more precisely, the stability at the different steady sates can be determined by calculating the eigenvalues of the matrix of the linearized model of the CSTR. If there is an eigenvalue with positive real part, the steady state is unstable, and all eigenvalues with negative real part indicates a stable steady state. Thus, by simulation it can be verified that the steady states P_1 and P_3 are stable and P_2 is unstable. This means that it is impossible to reach the point P_2 when the coolant flow rate is constrained.

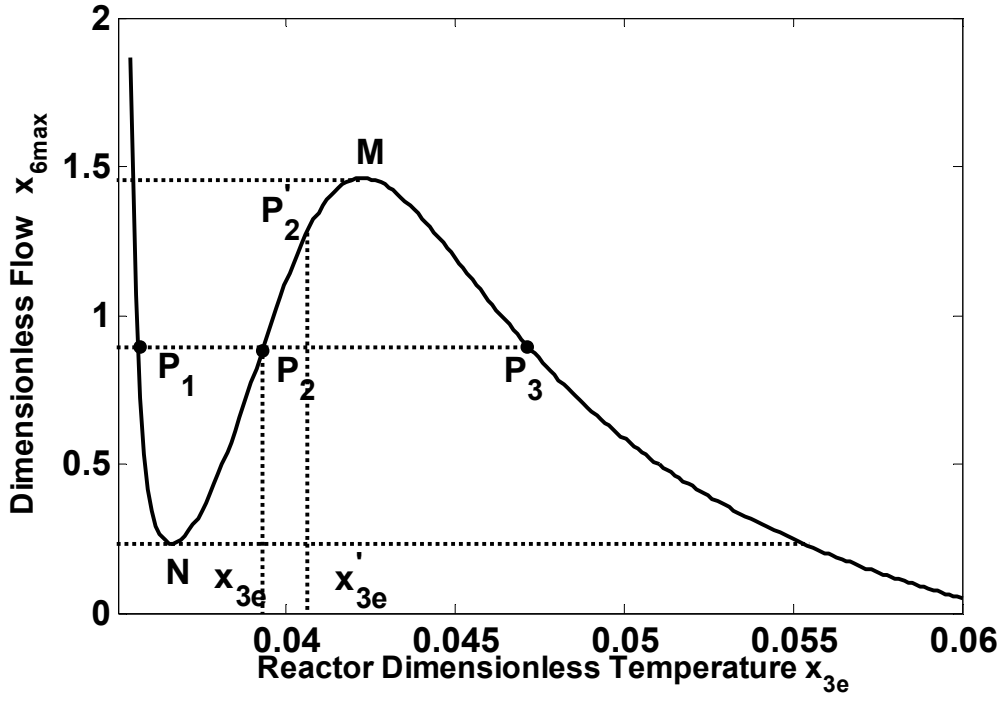

Figure 15. Dimensionless bifurcation plot when the coolant flow rate is constrained

The value of x_{6max} corresponding to the point M represents a global bifurcation. Thus, values of this flow above this point give a reactor behavior similar to case 3.1.1, i.e. when there is not limitation in the flow trough the control valve, and the control system can to drive the reactor to the desired set point. For values of x_{6max} under the corresponding to point N there is only one equilibrium point and this is the case 3.1.2, due to the low flow rate of cooling, the reactor temperature cannot reach the set point. In the next section, the study of chaotic behavior is carried out considering the R^4 and R^3 models of the reactor given by Eqs (34) and (35) respectively. Note that both R^3 and R^4 models have the same equilibrium points.

4.2. Analysis of the chaotic behavior

Consider the R^3 model defined by Eq (43). In order to obtain the equilibrium point at the origin (0,0,0), it will be is necessary to introduce the deviation variables given as:

$$x = x_2 - x_{2e} \;\; ; \;\; y = x_3 - x_{3e} \;\; ; \;\; z = x_6 - x_{6e} \tag{51}$$

So, Eqs. (43) can be rewritten as:

$$\left.\begin{aligned} \frac{dx}{d\tau} &= f_1(x,y,z) = x_{50}(x_{20} - (x + x_{2e})) - c_0 \cdot (x + x_{2e}) \cdot e^{-1/(y+x_s)} \\ \frac{dy}{d\tau} &= f_2(x,y,z) = x_{50}(x_{30} - (y + x_s)) + c_1 \cdot (x + x_{2e}) \cdot e^{-1/(y+x_s)} - \frac{c_2 c_3 sat(z + x_{6e})(y + x_s - x_{40})}{c_3 sat(z + x_{6e}) + c_4} \\ \frac{dz}{d\tau} &= f_3(x,y,z) = \frac{K_{td}}{x_{30}} \cdot \frac{dy}{d\tau} + \frac{K_{td}}{x_{30}\tau_{2d}} \cdot y \end{aligned}\right\} \tag{52}$$

where the sat() term is defined by Eq (42). Equations $f_i(x,y,z)$ can be expanded in series of Taylor up to first order approximation, so the linearized system at the origin can be written as:

$$\begin{bmatrix} \dot{x} \\ \dot{y} \\ \dot{z} \end{bmatrix} = \begin{bmatrix} -(x_{50} + c_0 e^{-1/x_s}) & -c_0 \frac{x_{2e}}{x_s^2} e^{-1/x_s} & 0 \\ c_1 e^{-1/x_s} & -x_{50} + c_1 \frac{x_{2e}}{x_s^2} e^{-1/x_s} - \frac{c_2 c_3 x_{6e}}{c_3 x_{6e} + c_4} & -\frac{c_2 c_3 (x_s - x_{40})}{(c_3 x_{6e} + c_4)^2} \\ \frac{K_{td}}{x_{30}} c_1 e^{-1/x_s} & \frac{K_{td}}{x_{30}} \left[-x_{50} + c_1 \frac{x_{2e}}{x_s^2} e^{-1/x_s} - \frac{c_2 c_3 x_{6e}}{c_3 x_{6e} + c_4} + \frac{1}{\tau_{2d}} \right] & \frac{K_{td}}{x_{30}} \left[-\frac{c_2 c_3 (x_s - x_{40})}{(c_3 x_{6e} + c_4)^2} \right] \end{bmatrix} \cdot \begin{bmatrix} x \\ y \\ z \end{bmatrix} \tag{53}$$

The eigenvalues of the linearized model R^3 given by Eq (53) can be deduced for a value of the set point temperature x_s, and the values of the PI controller as a function of the inlet dimensionless flow x_{50}. Note that the variables x_{50}, x_{20}, x_{30}, x_{40} can be considered as external disturbances, however only x_{50} will be considered as variable, whereas x_{20}, x_{30}, x_{40} are considered as constant.

Remark 4. Taking into account Eq (34), similar Eqs. to (51) and (52) can be obtained for R^4 model. Nevertheless both R^3 and R^4 models have the same equilibrium points.

In Figure 16, the variation of real part of eingenvalues vs. the volumetric flow rate inlet stream x_{50} , both R^3 and R^4 vector fields, when x_{20}, x_{30}, x_{40} remain constant, are shown. It can be observed that these values are close. This means that the jacket's dynamics can be considered negligible. It is clear that from a certain value of $x_{50} = F_0/F_{0s}$ there is an eigenvalues with real part positive, and so the equilibrium point will be unstable.

Consider the space state model R^3 defined by Eq (52), showing an equilibrium point such that the matrix of the linearized system at this point has a real negative eigenvalue λ and a pair of complex eigenvalues $\alpha \pm j.\beta$, ($j = \sqrt{-1}$) with positive real parts α. In this situation, the equilibrium point has one-dimensional stable manifold and two-dimensional unstable manifold. If the condition $\lambda < |\alpha|$ is verified, it is possible that an homoclinic orbit appears, which tends to the equilibrium point. This orbit is very singular, and then the Shilnikov theorem asserts that

every neighborhood of the homoclinic orbit contains infinite number of unstable periodic orbits.

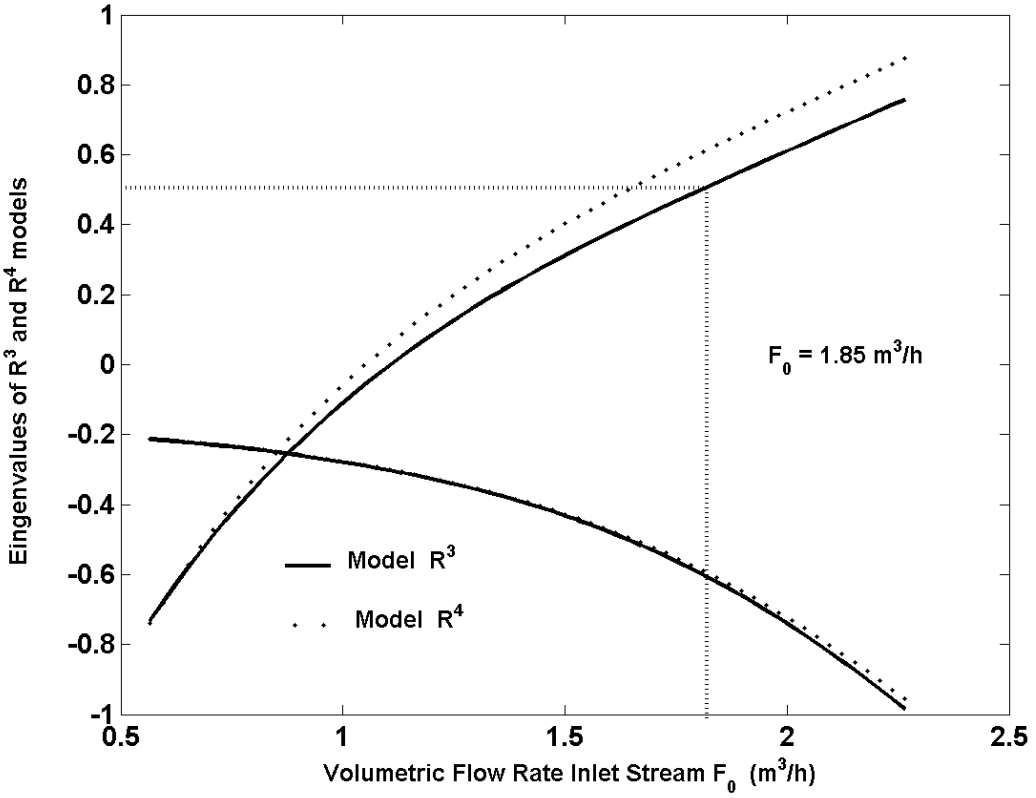

Figure 16. Real part of eigenvalues of the vector fields R^3 and R^4 vs. volumetric flow rate inlet stream F_0

The existence of the equilibrium point and the conditions for the eigenvalues of the linearized model are not difficult to find, nevertheless the hypothesis on the existence of a Shilnikov homoclinic orbit is usually very difficult to establish. For example, with a disturbance inlet flow rate of F_0 = 1.85 m^3/h, from Figure 16 the values of eigenvalues are: 0.5 ± 1.92.j ; -0.57, so the Jordan quasi-diagonal form is:

$$\Lambda = \begin{bmatrix} \rho & -\omega & 0 \\ \omega & \rho & 0 \\ 0 & 0 & \lambda \end{bmatrix} \; ; \; \lambda_{1,2} = \rho \pm \omega \cdot j \; ; \; \lambda_3 = \lambda \qquad (53)$$

If ρ, $\omega > 0$; $-\lambda > 0$ and $-\lambda/\rho > 1$ the equilibrium point is unstable, and a Shilnikov' orbit can appear. For the reactor, with a value of $x_{50} > 1$ and $x_{6max} \approx (x_{6max})_M$ (see Figure 15), by simulation it is possible to verify the presence of a homoclinic orbit to the equilibrium point. Figure 17 shows the homoclinic orbit for the model R^3 and R^4, when the steady state has been reached. Note that the Shilnikov orbit appear when the coolant flow rate is constrained. If there is no limitation of

the coolant flow rate, a limit cycle is obtained both in models R^3 and R^4, by simulation.

In accord with the Shilnikov's theorem, the reactor has a chaotic behavior. In order to test the presence of a strange attractor, it is necessary to raise the value of x_{6max} to introduce a perturbation in the vector field around the homoclinic orbit. Taking $x_{6max} = 5$, the results of the simulation are shown in Figure 18, where the sensitive dependence on initial conditions has been corroborated.

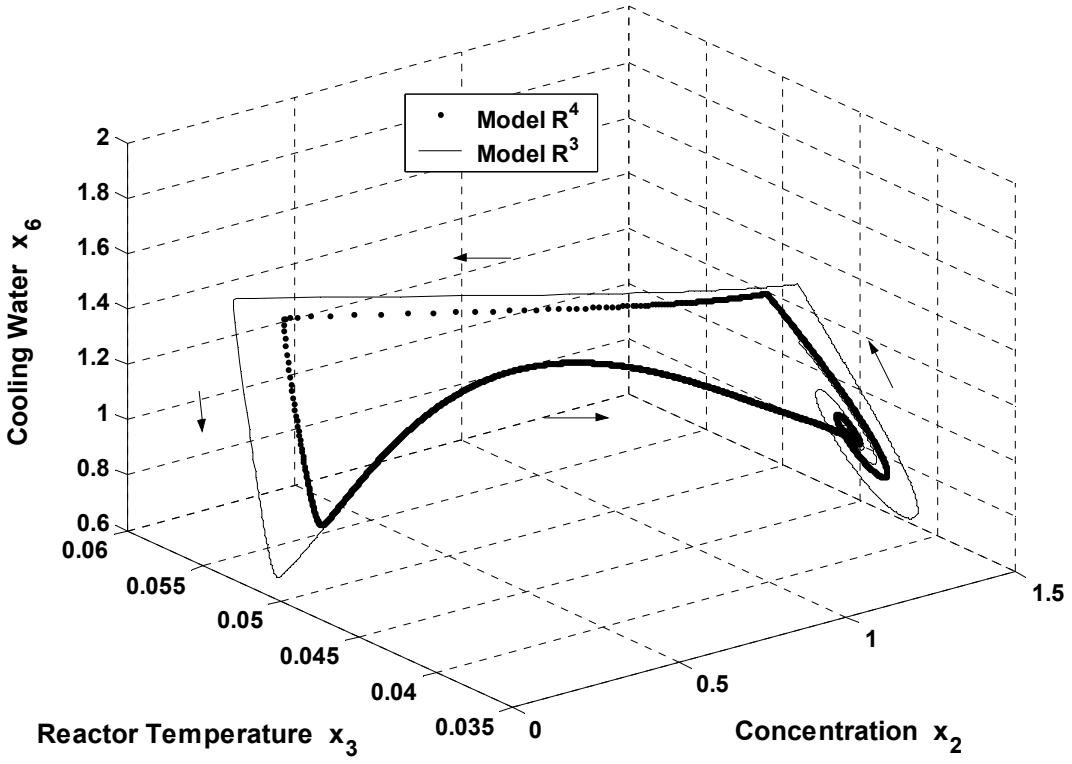

Figure 17. Homoclinic orbit of Shilnikov Type for the vector fields R^3 and R^4. Eigenvalues at the equilibrium point for R^3: $\lambda = -056$; $\alpha \pm \beta.j = 0.39 \pm 1.92.j$

It is interesting to note that in chaotic regime, the flow rate outlet stream, which is manipulated by the control valve CV1 (see Figure 12), and the reactor volume, are driven by the PI controller to the equilibrium point without chaotic oscillations. However, the other variables have a chaotic behavior as shown in Figure 18. So it is possible to obtain a reactor behavior, in which some variables are in steady state and the others are in regime of chaotic oscillations, due to the decoupling or serial connection phenomena. Thus the control system and the volumetric flow limitation of coolant flow rate through the

control valve VC2, are the responsible of this behavior. Similar results can be obtained from R^4 model.

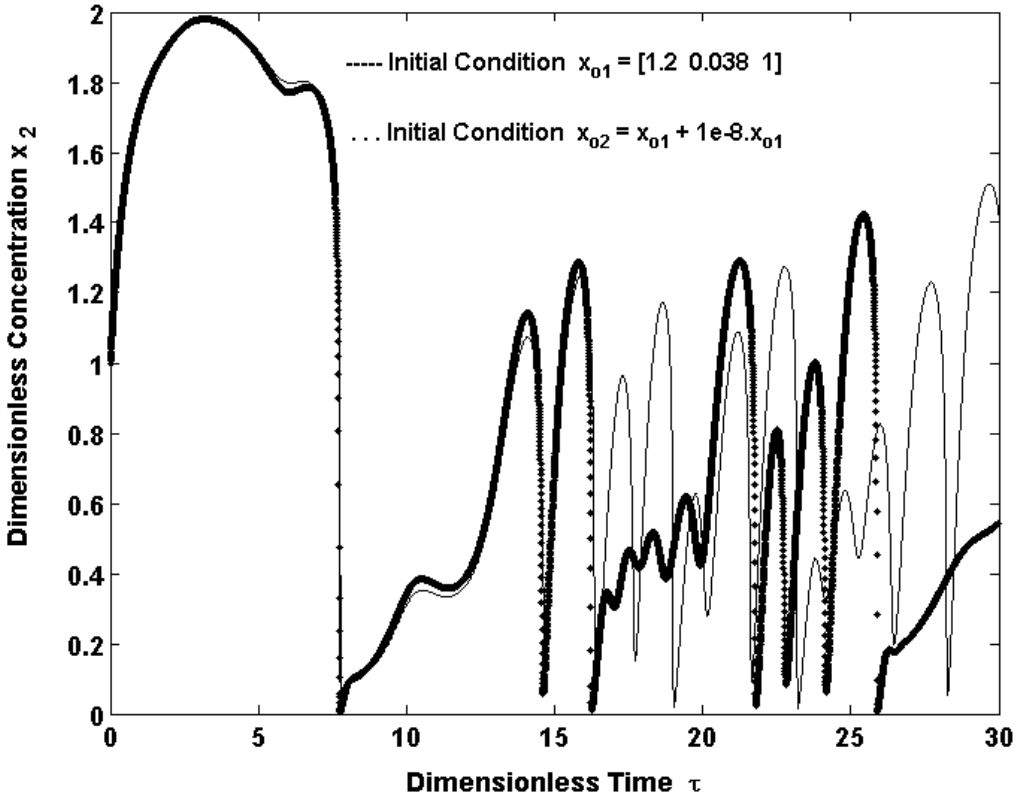

Figure 18. Sensitive dependence of the dimensionless concentration of R^3 model with two very close initial conditions. K_t = 0.094 m^3/h.°C; t_2 = 5 h.

Conclusions

From the study presented in this chapter, it has been demonstrated that a CSTR in which an exothermic first order irreversible reaction takes place, can work with steady-state, self-oscillating and chaotic dynamic. By using dimensionless variables, and taking into account an external periodic disturbance in the inlet stream temperature and coolant flow rate, it has been shown that chaotic dynamic can appear. This behavior has been analyzed from the Lyapunov exponents and the power spectrum.

Although this previously cited behavior is interesting, another more complicated case is researched from the analysis of the eingenvalues of the Eqs of the reactor linearized at the equilibrium point. In this case, it has been corroborated that the steady state can be modified throughout the variation of the composition and temperature of inlet stream to the reactor. From the parameters-plane inlet stream temperature-composition, the presence of various zones, i.e. a lobe and a

curve with cusp point, with different dynamical behavior has been shown. So, if the dimensionless concentration and temperature of the inlet flow rate to the reactor are inside the lobe, the reactor reaches a self-oscillating behavior. This self-oscillating dynamical behavior can be very difficult to obtain, because the area of the lobe is very small. When the reactor is in self-oscillating mode, applying an external periodic disturbance in the coolant flow rate, chaotic dynamics can appear. This chaotic behavior is very difficult to obtain with only an external periodic disturbance in the coolant flow rate.

The non-linear dynamics of the reactor with two PI controllers that manipulates the outlet stream flow rate and the coolant flow rate are also presented. The more interesting result, from the non-linear dynamic point of view, is the possibility to obtain chaotic behavior without any external periodic forcing. The results for the CSTR show that the non-linearities and the control valve saturation, which manipulates the coolant flow rate, are the cause of this abnormal behavior. By simulation, a homoclinic orbit at the equilibrium point of Shilnikov type has been found. In this case, chaotic behavior appears at and around the parameter values from which the previously cited orbit is generated.

From the results presented in this chapter, more advanced studies from the bifurcation theory can be planed. For example, inside the lobe, the behavior of the reactor is self-oscillating, i.e. an Andronov-Poincare-Hopf bifurcation can be researched from the calculation of the first Lyapunov value, in order to know if a weak focus can appear, or the conditions which give a Bogdanov-Takens bifurcation etc. Finally, it is interesting to remark that the previously analyzed phenomena should be known by the control engineer in order to either avoid them or use them, depending on the process type.

Appendix

The Lyapunov exponents provide a computable measure of the sensitivity to initial conditions, i.e. characterize the mean exponential rate of divergence of two nearby trajectories if there is at least one positive Lyapunov exponent, or convergence when all Lyapunov exponents are negative. The Lyapunov exponents are defined for autonomous dynamical systems are defined by:

$$\frac{dx_i(t)}{dt} = f_i\left[x_i(t)\right] \;;\; i = 1,2,...,n \Rightarrow \frac{dx(t)}{dt} = f\left[x(t)\right] \;;\; x(t) \in \boldsymbol{R}^n \qquad \text{(A-1)}$$

Consider a trajectory in the $\boldsymbol{R}^n$ n-dimensional space of $x(t)$ and a nearby trajectory $x(t) + \delta x(t)$, where the symbol δ means an infinitesimal variation, i.e. an arbitrary infinitesimal change not tangent to the initial trajectory. Eq (A-1) can be linearized throughout the trajectory to obtain

$$\frac{d\left[x(t) + \delta x(t)\right]}{dt} = f\left[x(t) + \delta x(t)\right] \qquad \text{(A-2)}$$

Now the function $f[x(t) + \delta x(t)]$ can be expanded in series up to first order term to give

$$f\left[x(t)+\delta x(t)\right]=f\left[x(t)\right]+\left(\frac{\partial f}{\partial x}\right)_{\delta x(t)=0}.\delta x(t) \qquad \text{(A-3)}$$

Substituting Eq (A-3) into Eq (A-2) the following linearized system throughout the trajectory is obtained:

$$\delta\dot{x}(t)=J\left[x(t)\right]\cdot\delta x(t) \qquad \text{(A-4)}$$

where the dot indicates differentiation respect to time and *J[x(t)]* is the jacobiam matrix of system (A-1).

The Lyapunov exponent of order one is defined by:

$$\lambda_i^1=\lim_{\substack{t\to\infty\\ \delta(x_0,0)\to 0}}\frac{1}{t}\ln\left(\frac{\delta(x_0,t)}{\delta(x_0,0)}\right)\ ;\ i=1,2,...,n \qquad \text{(A-5)}$$

This value is a measure of the mean exponential rate of divergence (convergence) of two initially very close trajectories, i.e. when $\delta(x_0,0)\to 0$. The values from (A-5) are the so called Lyapunov characteristic exponents, which can be ordered by size:

$$\lambda_1^1\geq\lambda_2^1\geq.....\geq\lambda_n^1 \qquad \text{(A-6)}$$

It is possible to generalize the previous concept to describe the mean rate of exponential growth (decrease) of a m-dimensional volume in the tangent space of $\boldsymbol{R^n}$, where m ≤ n. The Lyapunov exponent of order *m* is defined as

$$\lambda^m=\lim_{t\to\infty}\frac{1}{t}\log_2\left(\frac{V_m(t)}{V_m(0)}\right)\ ;\ m=1,2,...,n \qquad \text{(A-7)}$$

where:

$$V_m=\delta\vec{x}_1\wedge\delta\vec{x}_2\wedge....\wedge\delta\vec{x}_m \qquad \text{(A-8)}$$

is the volume of an m-dimensional parallelepiped whose edges are $\delta\vec{x}_1,\delta\vec{x}_2,....,\delta\vec{x}_m$. Then, the Lyapunov exponent associated to the direction *m* is defined as:

$$\lambda_m=\lambda^m-\lambda^{m-1} \qquad \text{(A-9)}$$

In order to determine λ_m, the values of Lyapunov exponents or order *m* must be known and consequently, using Eqs. (A-7) and (A-8), it will be necessary to integrate Eq (A-4). However, this Eq presents numerical problems because the divergence of nearby trajectories can be very strong (In chaotic dynamic this phenomenon is known as stretching and folding), and the linearization process is numerically unstable. This problem is overcome by using the orthonormalization Gram-Schmidt procedure. This is the idea of the method developed by Benettin et al.(1980).

The calculation of the Lyapunov exponents of order *m* has been carried out as follows. The following notation is useful:

$$\delta x_{k-1}^{j}(T)$$

where the superindex means the vector number, the subindex a generic integration step and *T* is the integration step used in the numerical algorithm. For example, $\delta x_{k-1}^{1}(T)$ means the vector one which comes from the vector $\delta x_{k-1}^{1}(0)$ as results of integration process of Eqs. (A-4) when the state of the non-linear system (A-1) has changed from *x[(k-1)T]* to *x[KT]*, i.e.

$$x\left[(k-1)T\right] \rightarrow x\left[kT\right] \Rightarrow \delta x_{k-1}^{1}(0) \rightarrow \delta x_{k-1}^{1}(T) \qquad \text{(A-10)}$$

When all $\delta x_{k-1}^{j}(T)\,; j=1,2,.,n$ are known, the Gram-Schmidt orthonormalization procedure is applied, so a new set of $\delta x_{k}^{j}(0)$ are obtained and a new iteration start. Once $\delta x_{k-1}^{j}(T)\,; j=1,2,...,n$ are known, the following Euclidian distances are calculated

$$d_k^j = \left\| \delta x_{k-1}^{j}(T) \right\| \;\; ; \; j=1,2,....,m \qquad \text{(A-11)}$$

Then, the Lyapunov exponent of order m is calculated from the Eq:

$$\lambda^m = \lim_{n\to\infty} \frac{1}{nT} \sum_{i=1}^{n} \log_2 \left(d_i^1 \cdot d_i^2 \cdot ....\cdot d_i^m \right) \qquad \text{(A-12)}$$

Taking into account Eq (A-9)the value of the Lyapunov exponent associated to the direction *m* is deduced as follows:

$$\lambda^m = \lim_{n\to\infty} \frac{1}{nT} \sum_{i=1}^{n} \log_2 d_i^m \qquad \text{(A-13)}$$

The Gram-Schmidt orthonormalization method is applied using the following steps.

i. The first value $\delta x_{k}^{j}(0)$ is defined by

$$\delta x_k^1(0) = \frac{\delta x_{k-1}^{1}(T)}{d_k^1} = \frac{\delta x_{k-1}^{1}(T)}{\left\| \delta x_{k-1}^{1}(T) \right\|} \qquad \text{(A-14)}$$

i.e. the normalized value of $\delta x_{k-1}^{j}(T)$. Now, the values of $\delta x_{k}^{j}(0)$ with $j=2,3,...,n$ must be calculated.

ii. Successively determine for *j = 2,3,...,n* the new variables:

$$v_{k-1}^{j}(T) = \delta x_{k-1}^{j}(T) - \sum_{i=1}^{j-1}\left[\delta x_{k}^{j}(0)\cdot\delta x_{k-1}^{j}(T)\right]\cdot\delta x_{k}^{j}(0)$$
$$d_{k}^{j} = \left\| v_{k-1}^{j}(T)\right\| \;\; ; \; j = 2,3,...,n \qquad \text{(A-15)}$$

iii. With the previously calculated value determine:

$$\delta x_{k}^{j} = \frac{v_{k-1}^{j}(T)}{d_{k}^{j}} \;\; ; \; j = 2,3,...,n \qquad \text{(A-16)}$$

The calculation process has been implemented by using a Matlab © program throughout the following steps.

1. From Eq (A-1) by using the Runge-Kutta or Runge-Kutta-Fehlberg intregration method the state variables *x(t)* can be calculated.

2. From the values *x(t)* the jacobian matrix *J[x(t)]* can be calculated. For example, in a system of order *n = 4*, four vectors of dimension four must be determined. To carry out this, a matrix of 16x16 elements is defined as follows:

$$JJ = \begin{bmatrix} J & Z & Z & Z \\ Z & J & Z & Z \\ Z & Z & J & Z \\ Z & Z & Z & J \end{bmatrix} \;\; ; \; J(4x4) \;\; ; \; Z = zeros(4x4) \qquad \text{(A-17)}$$

3. The R-K or R-K-F method is applied to the linear system

$$\frac{dz(t)}{dt} = JJ\cdot z(t) \qquad \text{(A-18)}$$

and the following values are obtaned:

$$\left.\begin{aligned} \delta x_1(1:4,i) &= z(1:4,i) \\ \delta x_1(5:8,i) &= z(5:8,i) \\ \delta x_1(9:12,i) &= z(9:12,i) \\ \delta x_1(12:16,i) &= z(12:16,i) \end{aligned}\right\} \qquad \text{(A-19)}$$

4. From Eqs. (A-19) the Gram-Schmidt orthonormalization is applied to obtain the normalized values $\left[\delta x_{1n}, \delta x_{2n}, \delta x_{2n}, \delta x_{2n}\right]$. The following integration step is carried out with the values:

$$z(1:16, i+1) = \left[\delta x_{1n}; \delta x_{2n}; \delta x_{2n}; \delta x_{2n}\right] \qquad \text{(A-20)}$$

5. From the normalized vector $\left[\delta x_{1n}, \delta x_{2n}, \delta x_{2n}, \delta x_{2n}\right]$ the four Lyapunov exponents are calculated as follows

$$S_1 = \left[d_1; d_2; d_3; d_4 \right] \;;\; S_2 = \log_2 \left(S_1 \right) \;;\; S = S + S_2$$
$$NL(1:4,i) = \frac{S}{t(i)} \qquad \text{(A-21)}$$

where *S* is an accumulative auxiliary variable and *t(i)* is the value of the integration time.

References

Albertos, P. Pérez Polo, M. (2005) Nonisothermal stirred-tank reactor with irreversible exothermic reaction A → B. 1.Modelling and local control (to appear). Springer-Verlag

Alvarez-Ramirez, J., Femat, R., Gonzalez-Trejo, J. (1998). Robust control of a class of uncertain first-order systems with least prior knowledge, Chem. Eng. Sci. 53 (15) 2701-2710.

Alvarez-Ramirez, J., Suarez, R., Femat, R. (1997). Robust stabilization of temperature in continuous-stirred tank reactors, Chem. Eng. Sci. 52 (14) 2223-2230.

Andronov, A. A., Vitt, A. A., Khaikin, S. E. (1966). Theory of Oscillations. Pergamon Press. Oxford.

Benettin, G, Galgani, L., Strelcyn, J-M, (1980) "Lyapunov characteristic exponents for smoth dynamical systems and for Hamiltonian systems: a method for computing all of them". *Meccanica,* Vol. 15, pp 9-20.

Benettin, G, Galgani, L., Strelcyn, J-M, (1980) "Lyapunov characteristic exponents for smoth dynamical systems and for Hamiltonian systems: a method for computing all of them". *Meccanica,* Vol. 15, pp 21-30.

Cartwright, M.L., & Littlewood, J.E. (1945). On nonlinear differential equations of the second order,I: The equation: $\ddot{y} + k(1 - y^2)\dot{y} + y = b\lambda\cos(\lambda t + a)$, k large. Lond. Math. Soc. 20, 180-189.

Dolnik, M., Banks, A. S., Epstein, I.R. (1997). Oscillatory chemical reaction in a CSTR with feedback control of flow rate, Journal Phys. Chem. A 101 5148-5154.

Femat, R. (2000). Chaos in a class of reacting systems induced by robust asymptotic feedback, Physica D. 136 193-204.

Glendinning, P. (1994). Stability, instability and chaos: an introduction to the theory of nonlinear differential equations. Cambridge University Press.

Guckenheimer, J., & Holmes, P. (1983). Nonlinear Oscillations, Dynamical Systems, and Bifurcations of Vector Fields. Springer-Verlag, New York.

Hopf, E. (1942). Abzweigung einer periodischen Lösung von einer stationaren Lösung eines Differetiasystems. *Ver Math.-Phys. Kl. Sachs, Acad Wiss. Leipzig* 94, 1-22.

Kevrekidis, G., Aris, R. & Schmidt, L.D. (1986). The Stirred Tank Forced. *Chem. Eng. Sci.* 41(6), 1549-1560.

Kubickova, Z., Kubicek, M. Marek, M. Feed-batch operation of stirred reactors, Chem. Eng. Sci. 42 (2) (1987) 327-333.

Kurtz, M.J., Yan Zhu, G., & Henson, M.A. (2000). Constrained Ouput Feedback Control of a Multivariable Polymerization Reactor. IEEE Trans. Control Syst. Tech. 8, 87-97.

Lichtenberg, A.J., & Lieberman, M.A. (1992). Regular and Chaotic Dynamics, 2nd ed. Springer-Verlag, New York.

Mankin J.C. & Hudson, J.L. (1984). Oscillatory and Chaotic Behaviour of a Forced Exothermic Chemical Reaction. *Chem. Eng. Sci.* 39(12), 1807-1814.

Marsden J. E. & McCraken M. (1976). *The Hopf Bifurcation and its Applications*. Springer, New York.

Ott E. (2002). Chaos in Dynamical Systems. Cambridge University Press.

Pellegrini, L., Biardi, G. Chaotic behaviour of a controlled CSTR, Computers Chem.Engng. 14 (1990) 1237-1247.

Pérez, M. Font, R., Montava, M.A. (2002). Regular self-oscillating and chaotic dynamics of a continuous stirred tank reactor. *Computers & Chem. Eng.* 26. 889-901.

Pérez M., Albertos, P. (2004) Self-oscillating and chaotic behaviour of a PI-controlled CSTR with control valve saturation. *Journal of Process Control*. 14, 51-59.

Planeaux, J.B. & Jensen, K.F. (1986). Bifurcation Phenomena in CSTR Dynamics: A System with Extraneous Thermal Capacitance. *Chem. Eng. Sci.* 41(6), 1497-1523.

Seydel R. (1994). Practical Bifurcation and Stability Analysis From Equilibrium to Chaos, 2nd ed. Springer-Verlag, New York.

Shilnikov, L.P. (1965). A case of the existence of a demensurable set of periodic motions. Sov. Math. Dokl. 6, 163-166.

Shilnikov, L. P., Shilnikov, A. L., Turaev, P. V., Chua, O. L.(2001). Methods of qualitative theory in nonlinear dynamics. Part II. World Scientific. Series in Nonlinear Science.

Soroush, M. (1997). Nonlinear state-observer design with application to reactors. Che. Eng. Sci. 52(3), 387-404.

Teymour, F. & Ray W.H. (1989). The Dynamic Behavior of Continuous Solution Polymerization Reactors-IV. Dynamic Stability and Bifurcation Analysis of an Experimental Reactor. Chem. Eng. Sci. 44(9), 1967- 1982.

Teymour, F. (1997) Dynamics of Semibatch Polymerization Reactors: I. Theoretical Analysis. AIChE J. 43(1), 145-156.

Tomita, K. (1986) Periodically forced nonlinear oscillators. *Chaos, ed A.V. Holden, Princenton Univ. Press,* 211-236.

Uppal, Y., Ray, W.H., Poore, A.B. (1974). On the dynamic behavior of continuous stirred tank reactors. *Chem. Eng. Sci.* 29, 967-985.

Vaganov, D.A., Samoilenko N.G. & Abranov, V.G. (1978). Periodic Regimes of Continuous Stirred tank Reactors. Chem. Eng. Sci. 33, 1133-1140.

Wiggins, S. (1988). Global Bifurcations and Chaos.Springer. New York

Wiggins, S. (1990) *Introduction* to Applied Nonlinear Dynamical System and Chaos. Springer, New York.

Zhabotinsky, A.M., Rovinskii, A.B. (1984). Self-Organization, Autowaves and Structures Far from Equilibrium. Springer, Berlin.